

ARTICLE

Received 9 May 2016 | Accepted 19 Apr 2017 | Published 5 Jun 2017

DOI: 10.1038/ncomms15663

OPEN

# The ATP-binding cassette transporter A1 regulates phosphoantigen release and V $\gamma$ 9V $\delta$ 2 T cell activation by dendritic cells

Barbara Castella<sup>1,2,\*</sup>, Joanna Kopecka<sup>3,\*</sup>, Patrizia Sciancalepore<sup>1,2</sup>, Giorgia Mandili<sup>1,4</sup>, Myriam Foglietta<sup>1,2</sup>, Nico Mitro<sup>5</sup>, Donatella Caruso<sup>5</sup>, Francesco Novelli<sup>1,4</sup>, Chiara Riganti<sup>2,3,\*\*</sup> & Massimo Massaia<sup>1,2,4,6,\*\*</sup>

V $\gamma$ 9V $\delta$ 2 T cells are activated by phosphoantigens, such as isopentenyl pyrophosphate (IPP), which is generated in the mevalonate pathway of antigen-presenting cells. IPP is released in the extracellular microenvironment via unknown mechanisms. Here we show that the ATP-binding cassette transporter A1 (ABCA1) mediates extracellular IPP release from dendritic cells (DC) in cooperation with apolipoprotein A-I (apoA-I) and butyrophilin-3A1. IPP concentrations in the supernatants are sufficient to induce V $\gamma$ 9V $\delta$ 2 T cell proliferation after DC mevalonate pathway inhibition with zoledronic acid (ZA). ZA treatment increases ABCA1 and apoA-I expression via IPP-dependent LXR $\alpha$  nuclear translocation and PI3K/Akt/mTOR pathway inhibition. These results close the mechanistic gap in our understanding of extracellular IPP release from DC and provide a framework to fine-tune V $\gamma$ 9V $\delta$ 2 T cell activation via mevalonate and PI3K/Akt/mTOR pathway modulation.

<sup>1</sup>Dipartimento di Biotecnologie Molecolari e Scienze della Salute, Università degli Studi di Torino, Via Nizza 52, Torino 10126, Italy. <sup>2</sup>Centro di Ricerca in Medicina Sperimentale (CeRMS), AOU Città della Salute e della Scienza di Torino, Via Santena 5, Torino 10126, Italy. <sup>3</sup>Dipartimento di Oncologia, Università degli Studi di Torino, Via Santena 5/bis, Torino 10126, Italy. <sup>4</sup>Centro Interdipartimentale di Ricerca per le Biotecnologie Molecolari (CIRBM), Via Nizza 52, Torino 10126, Italy. <sup>5</sup>Dipartimento di Scienze Farmacologiche e Biomolecolari, Università degli Studi di Milano, Via Balzaretti 9, Milano 20133, Italy.

<sup>6</sup>SC. Ematologia, AO S. Croce e Carle, Via Michele Coppino 26, Cuneo 12100, Italy. \* These authors contributed equally to this work. \*\* These authors jointly supervised this work. Correspondence and requests for materials should be addressed to C.R. (email: chiara.riganti@unito.it) or to M.M. (email: massimo.massaia@unito.it).

**V** $\gamma$ 9V $\delta$ 2 T cells are activated by phosphoantigen that are generated in the mevalonate and non-mevalonate pathway of microbial pathogens. The mevalonate pathway of mammalian cells also generates phosphoantigens such as isopentenyl pyrophosphate (IPP), which activate V $\gamma$ 9V $\delta$ 2 T cells almost as efficiently as microbial phosphoantigens<sup>1,2</sup>. V $\gamma$ 9V $\delta$ 2 T cells recognize tumour cells that release mevalonate pathway-derived phosphoantigens as IPP<sup>1</sup>. In addition, V $\gamma$ 9V $\delta$ 2 T cells are specifically activated by antigen-presenting cells, such as dendritic cells (DC), particularly when intracellular IPP generation is boosted with zoledronic acid (ZA), which is an inhibitor of the farnesyl pyrophosphate synthase (FPPS) in the mevalonate pathway<sup>3–5</sup>. How IPP is released in the extracellular microenvironment and delivered to V $\gamma$ 9V $\delta$ 2 T cells is unknown.

CD277/butyrophilin-3A1 (BTN3A1) is a type I glycoprotein that has a central function in phosphoantigen-induced V $\gamma$ 9V $\delta$ 2 T cell activation (reviewed in Harly *et al.*)<sup>4</sup>. Two mechanisms have been hypothesized: the ‘allosteric model’ proposed by Harly *et al.*<sup>6</sup> and ‘antigen-presenting model’ by Vavassori *et al.*<sup>7</sup> In the first model, the interaction between intracellular phosphoantigens and the intracellular B30.2 domain of BTN3A1 induces conformational changes of the extracellular domain, which are sensed by V $\gamma$ 9V $\delta$ 2 T cells and cause their activation. In Vavassori’s model, intracellular phosphoantigens are exported to the extracellular microenvironment by an unidentified plasma-membrane-associated transporter and presented to V $\gamma$ 9V $\delta$ 2 T cells by the BTN3A1 extracellular domain. Most data currently available are in favour of the allosteric model<sup>8,9</sup>, but it is currently unknown whether BTN3A1 is also involved in extracellular phosphoantigen release.

Ecto-F1-ATPase and apolipoprotein A-I (apoA-I) are additional important molecules involved in V $\gamma$ 9V $\delta$ 2 T cell activation<sup>10–13</sup>. F1-ATPase can bind both apoA-I and triphosphoric acid 1-adenosin-59-yl ester 3-(3-methylbut-3-enyl) ester (ApppI), which is an adenylated derivative of IPP that accumulates in ZA-treated cells. IPP can be released from ApppI by nucleotide pyrophosphatase causing the activation of V $\gamma$ 9V $\delta$ 2 T cells<sup>11</sup>. Soluble apoA-I can improve V $\gamma$ 9V $\delta$ 2 T cell recognition of tumour cells, which overproduce IPP (that is, after ZA treatment), whereas low levels of circulating apoA-I in chronic inflammation are associated with a low activation state of V $\gamma$ 9V $\delta$ 2 T cells<sup>11–13</sup>.

apoA-I is required for the assembly of nascent high-density lipoprotein (HDL) particles, which mediate the reverse cholesterol transport<sup>14</sup>. apoA-I binds the extracellular domain of the ATP-binding cassette transporter A1 (ABCA1). ABCA1 is a member of the ABC transmembrane transporter family, which is abundant in the liver, the gastrointestinal tract and macrophages. ABCA1 effluxes cholesterol and phospholipids to lipid-poor/lipid-free apoA-I. During the HDL assembly process, ABCA1 cooperates with the ATP-binding cassette transporter G1 (ABCG1) and the scavenger receptor-BI (SR-BI), which are two transporters that are involved in the delivery of cholesterol and choline-rich phospholipids to HDL<sup>14</sup>. Interestingly, ABCA1 also effluxes  $\alpha$ -tocopherol<sup>15</sup>, which is a molecule that contains multiple isoprenoid units; however, it has never been reported whether ABCA1 or any other ABC transporter are involved in the extracellular release of IPP or other isoprenoids.

On the basis of these observations, here we test the hypothesis that ABCA1, apoA-I, and BTN3A1 are involved in extracellular IPP release. We demonstrate that ABCA1, in cooperation with apoA-I and BTN3A1, has a major function in extracellular IPP release from ZA-treated DC. Supernatants from ZA-treated DC contain sufficient IPP to induce V $\gamma$ 9V $\delta$ 2 T cell proliferation even after removal of ZA-treated DC. These data show that

ABCA1 has a function that may alter our understanding of the relationship between lipid metabolism and immune function.

## Results

**Soluble IPP-induced V $\gamma$ 9V $\delta$ 2 T cell proliferation.** Figure 1a shows the proliferation of V $\gamma$ 9V $\delta$ 2 T cells after 7-day stimulation of peripheral blood mononuclear cells (PBMC) from healthy donors with supernatants obtained from autologous monocytes (CD14+) or DC that are left untreated or treated with ZA for 24 h. As previously reported, supernatants from ZA-treated DC induced significant V $\gamma$ 9V $\delta$ 2 T cell proliferation<sup>5</sup>.

In a second set of experiments, DC were incubated for 24 h with or without ZA and washed to clear supernatants from any residual ZA. Washed DC were re-plated for an additional 24 and 48 h in the absence of any other treatment, and intracellular and extracellular IPP levels were evaluated as previously reported (Fig. 1b)<sup>3</sup>. ZA-treated washed DC released significant amounts of IPP for the first 24 h and their supernatants induced a dose-dependent proliferation of V $\gamma$ 9V $\delta$ 2 T cells (Fig. 1c).

The same set of experiments was performed using unmanipulated or DC-like cells that were generated from the acute monocytic leukaemia THP-1 cell line (DC<sup>THP1</sup>) and the histiocytic lymphoma U937 cell line (DC<sup>U937</sup>)<sup>16–18</sup>. DC<sup>THP1</sup> and DC<sup>U937</sup> have been shown to perform in many functional assays as well as the conventional counterparts generated from CD14+ cells. ZA-treated THP-1 cells and DC<sup>THP1</sup> produced significant amounts of intracellular IPP, such as ZA-treated DC (Fig. 1b), whereas U937 cells and DC<sup>U937</sup> produced lower amounts, which were unaffected by ZA treatment (Fig. 1d). Extracellular IPP release showed an opposite pattern: THP-1 cells and DC<sup>THP1</sup> did not release extracellular IPP even after ZA treatment, whereas ZA-treated DC<sup>U937</sup> released intermediate levels (Fig. 1d) that were similar to the levels released by ZA-treated DC (Fig. 1b). The different IPP concentrations in the supernatants translated into a different ability to induce V $\gamma$ 9V $\delta$ 2 T cell proliferation (Fig. 1e).

## Increased ABCA1 and apoA-I expression after ZA treatment.

ABCA1, ABCG1 and SR-BI expression were investigated under baseline conditions and after ZA treatment (Fig. 2a). THP-1, U937 and CD14+ cells exhibited no detectable ABCA1 or ABCG1 levels, irrespective of ZA treatment. ZA-treated DC<sup>THP1</sup> also exhibited no expression, whereas untreated DC<sup>U937</sup> and DC already exhibited detectable ABCA1 expression, which increased after ZA treatment. DC were the only cells to show detectable ABCG1 expression, which was upregulated by ZA treatment. SR-BI expression was uniformly detectable in all cell preparations and unaffected by ZA treatment. Pooled data with statistical analyses are shown in Fig. 2b.

apoA-I binds to the extracellular domain of ABCA1 to load cholesterol and phospholipids that are released in the reverse cholesterol transport. apoE is also involved in the same process but it binds to ABCG1. We performed a matrix-assisted laser desorption ionization-time-of-flight/mass spectrometry (MALDI-TOF/MS) analysis to investigate whether apoA-I and apoE were present in the supernatant of CD14+ cells and DC (Supplementary Table 1). Two bands of 36.1 and 30.7 kD, which correspond to apoE and apoA-I, were identified (Fig. 2c, left; Supplementary Fig. 1; Supplementary Table 1). ZA treatment did not modify apoE levels, whereas it increased apoA-I expression (Fig. 2c, right). These data indicate that ZA-induced mevalonate pathway inhibition increases the extracellular release of both IPP and apoA-I in both CD14+ and DC.

To further explore the relationship among IPP, apoA-I, and apoE, extracellular IPP was quantified in the supernatant of

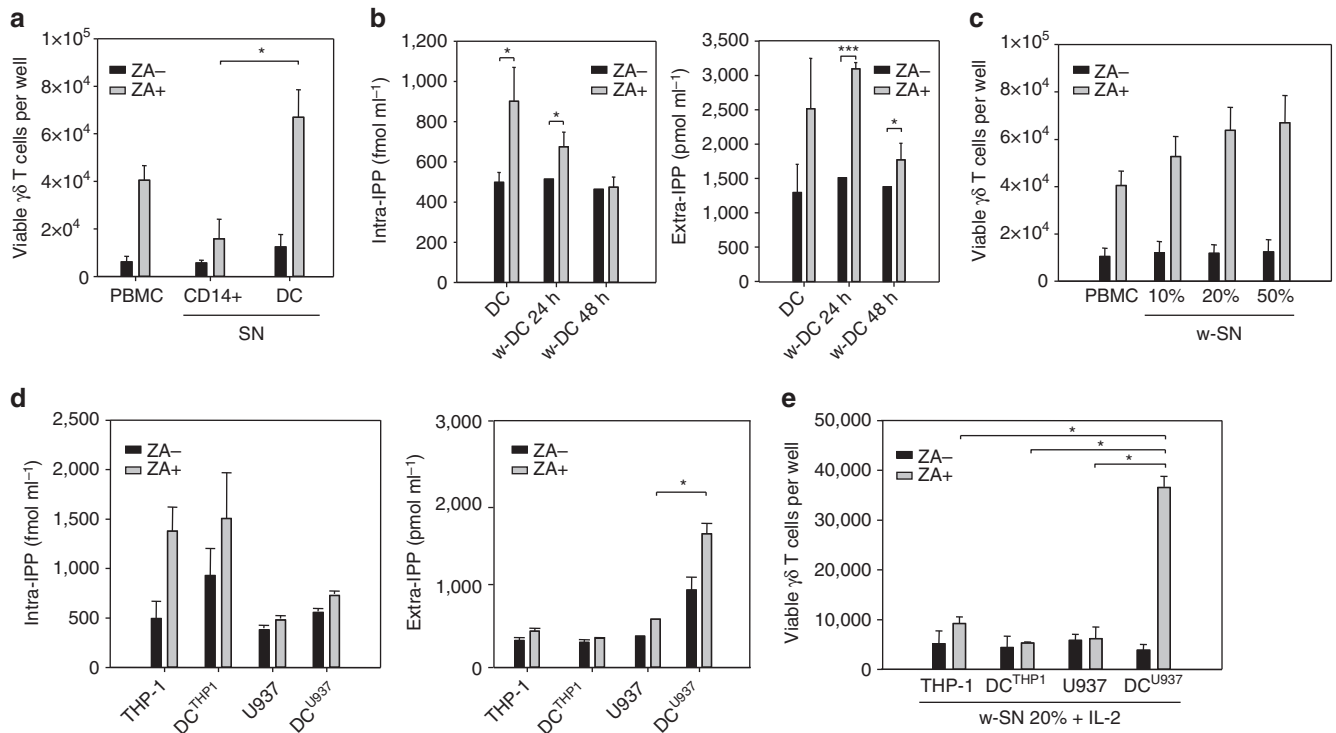


**Figure 1 | V $\gamma$ 9V $\delta$ 2 T cell proliferation is induced by extracellular IPP.** (a) V $\gamma$ 9V $\delta$ 2 T cell proliferation after 7-day PBMC stimulation with ZA or supernatant (SN) retrieved from untreated (ZA-) and ZA-treated (ZA+) CD14+ cells and DC. Supernatant from ZA-treated DC induced significantly higher V $\gamma$ 9V $\delta$ 2 T cell proliferation than PBMC stimulation with supernatant from ZA-treated CD14+ cells (\* $P$ <0.05; Wilcoxon-Mann-Whitney). The bars represent the mean value  $\pm$  s.e.m. of eight experiments. (b) Intracellular IPP concentrations in untreated (ZA-) and ZA-treated (ZA+) washed DC (w-DC) and extracellular IPP concentrations in corresponding SN after washing and incubation for 24 and 48 h without further ZA stimulation. ZA-treated w-DC released significant IPP amounts for 24 h after ZA removal. The bars represent the mean value  $\pm$  s.e.m. of ten experiments (\* $P$ <0.05; \* $P$ <0.001; ANOVA). (c) V $\gamma$ 9V $\delta$ 2 T cell proliferation after 7-day PBMC stimulation with ZA or with serial dilutions of supernatants (w-SN) retrieved from untreated (ZA-) and ZA-treated (ZA+) w-DC. The bars represent the mean value  $\pm$  s.e.m. of eight experiments. (d) Intracellular and extracellular IPP levels generated in untreated (ZA-) and ZA-treated (ZA+) THP-1 cells, DC<sup>THP1</sup>, U937 cells and DC<sup>U937</sup>. ZA-treated THP-1 cells and DC<sup>THP1</sup> generated high amounts of intracellular IPP, which was not released in the supernatant. Conversely, ZA-treated DC<sup>U937</sup> released extracellular IPP amounts that were close to the extracellular IPP amounts released by ZA-treated DC. Bars represent the mean value  $\pm$  s.e.m. of eight experiments (\* $P$ <0.05; ANOVA). (e) V $\gamma$ 9V $\delta$ 2 T cell proliferation after 7-day PBMC stimulation with supernatant obtained from untreated (ZA-) and ZA-treated (ZA+) THP-1 cells, DC<sup>THP1</sup>, U937 cells and DC<sup>U937</sup>. Only SN from ZA-treated DC<sup>U937</sup> induced V $\gamma$ 9V $\delta$ 2 T cell proliferation. The bars represent the mean value  $\pm$  s.e.m. of five experiments (\* $P$ <0.05; Wilcoxon-Mann-Whitney). ANOVA, analysis of variance.

untreated and ZA-treated THP-1 cells, U937 cells, CD14+ cells, DC<sup>THP1</sup>, DC<sup>U937</sup>, and DC after incubation with recombinant human apoA-I and apoE and pulsing with [<sup>14</sup>C]-IPP. As shown in Fig. 2d, exogenously added apoA-I and apoE promoted extracellular IPP release only in cells with detectable ABCA1 expression, that is, untreated and ZA-treated DC<sup>U937</sup> and DC.

To further build on the relationship between IPP and ABCA1, we correlated intracellular and extracellular IPP levels with ABCA1, ABCG1 and SR-B1 expression in a series of haematologically derived neoplastic and non-neoplastic cells (Supplementary Fig. 2A, Supplementary Fig. 2B). A strong correlation was detected between ABCA1 levels and extracellular IPP levels ( $r^2 = 0.98$ ), whereas no correlation between intracellular IPP levels and ABCA1 levels was identified (Supplementary Fig. 2C). ZA treatment upregulated ABCA1 expression only in cells with detectable ABCA1 under baseline conditions, such as the myeloma cell line SKMM1, primary multiple myeloma cells (CD138+ MM) and bone marrow stromal cells (BMSC) derived from multiple myeloma patients (Supplementary Fig. 3).

To eliminate the possibility that ZA-induced ABCA1 upregulation was not merely due to modifications of cholesterol content in the plasma-membrane and associated with non-specific changes in other membrane proteins, we compared the expression levels and

activities of unrelated transporters and channels in untreated and DC treated with ZA and/or simvastatin. Simvastatin is a selective inhibitor of 3- $\beta$ -hydroxy- $\beta$ -methylglutaryl coenzyme A reductase (HMGR) upstream to FPPS in the mevalonate pathway that strongly reduces cholesterol synthesis<sup>3</sup>. The results in Fig. 3 indicate that neither the expression nor the activity of other ABC transporters that are involved in cholesterol and lipid metabolites efflux (ABCA2, ABCB1, ABCC1, ABCC2, ABCC3, ABCC4, ABCC5, ABCC6, ABCG2, ABCG4, ABCG5, ABCG8), phosphate transporters potentially involved in pyrophosphate transport (PiT-1/SLC20A1, PiT-2/SLC20A2, NPT2A/SLC34A1), and other ubiquitous and unrelated pumps or channels (Na<sup>+</sup>/K<sup>+</sup>-ATPase, Na<sup>+</sup>/H<sup>+</sup> exchanger 1/NHE1, Cl<sup>-</sup>/HCO<sub>3</sub><sup>-</sup> transporter/SLC4A1) were modified by ZA or simvastatin treatment.

**IPP is released by ABCA1 in cooperation with BTN3A1.** Probuco is a functional ABCA1 inhibitor<sup>19</sup>. Probuco incubation of untreated and ZA-treated DC for 24 h marginally increased intracellular IPP levels and completely abrogated ZA-induced extracellular IPP release (Fig. 4a).

To confirm the role of ABCA1, siRNA were employed to silence *Abca1* in untreated and ZA-treated DC. The efficacy

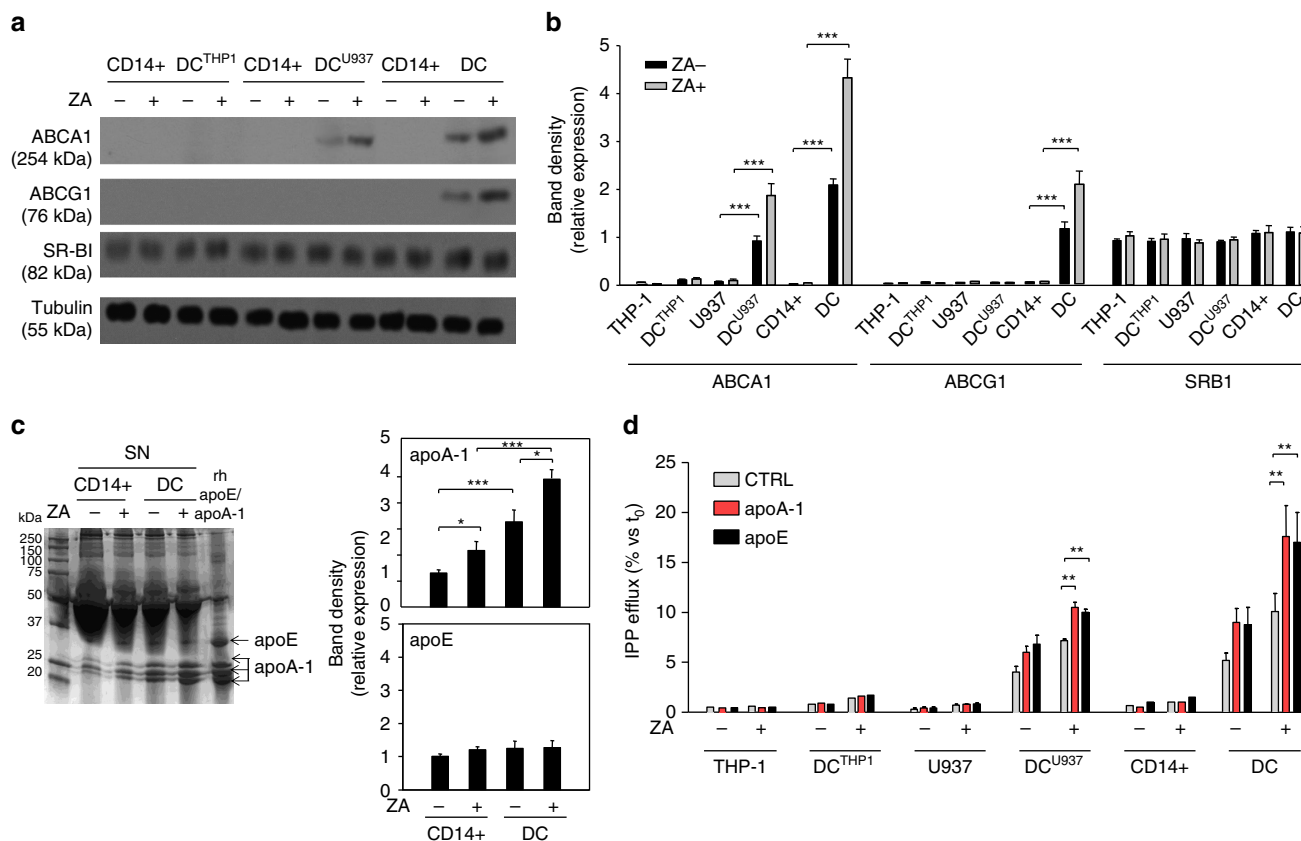


**Figure 2 | ZA treatment increases ABCA1 and apoA-1 expression.** (a) Western blot analysis of ABCA1, ABCG1 and SR-BI expression in untreated (ZA-) and ZA-treated (ZA+) THP-1 cells, U937 cells, CD14+ cells and corresponding DC subsets (DC<sup>THP1</sup>, DC<sup>U937</sup>, DC). ABCA1 was already detectable in DC<sup>U937</sup> and DC and its expression was upregulated by ZA.  $\beta$ -tubulin was employed to check the equal protein loading per lane. The results are obtained from one representative experiment of three experiments. (b) Pooled data obtained by densitometric analysis with ImageJ software (<http://imagej.nih.gov/ij/>). The results are expressed as arbitrary units (THP-1 cells and DC<sup>THP1</sup>,  $n=3$ ; U937 cells and DC<sup>U937</sup>,  $n=3$ ; CD14+ cells and DC,  $n=14$ ) ( $***P<0.001$ ; ANOVA). (c) Supernatants from untreated (ZA-) or ZA-treated (ZA+) CD14+ cells and DC were resolved by SDS-PAGE and stained with Coomassie brilliant blue. A concentration of  $1\ \mu\text{g ml}^{-1}$  recombinant human apoE or apoA-I were employed as standards. Densitometric analyses of bands identified as apoE or apoA-I by MALDI-TOF/MS were performed with ImageJ software. The results are expressed as arbitrary units. The gel is representative of one out of the three experiments ( $*P<0.05$ ,  $***P<0.001$ ; ANOVA). (d) Extracellular IPP released in the supernatants retrieved from untreated (ZA-) or ZA-treated (ZA+) CD14+ cells, U937 cells, THP-1 cells and corresponding DC subsets (DC, DC<sup>U937</sup>, DC<sup>THP1</sup>) in the absence (CTRL) or presence of human recombinant  $1\ \mu\text{g ml}^{-1}$  apoA-I or apoE added during the last 24 h of incubation. apoA-I and apoE increased the IPP release in DC and DC<sup>U937</sup> but did not increase the IPP release in DC<sup>THP1</sup>. The bars represent the mean value  $\pm$  s.e.m. of three experiments ( $**P<0.01$ ; ANOVA). ANOVA, analysis of variance. MALDI-TOF/MS, matrix-assisted laser desorption ionization-time-of-flight/mass spectrometry. SDS-PAGE: sodium dodecyl sulfate-polyacrylamide gel electrophoresis.

and specificity are shown in Fig. 4b. As expected, *Abca1*-silencing marginally increased intracellular IPP generation, whereas it completely abrogated ZA-induced extracellular IPP release (Fig. 4c). The inability to induce  $V\gamma 9V\delta 2$  T cell proliferation provided the functional demonstration that supernatants from ZA-treated *Abca1*-silenced DC were devoid of IPP (Fig. 4d). These results indicate that ABCA1 has a major role in the extracellular IPP release from ZA-treated DC.

BTN3A1 has been reported to be involved in the phosphoantigen-induced activation and recognition of target cells by  $V\gamma 9V\delta 2$  T cells<sup>5,6</sup>. To explore any relationship between ABCA1 and BTN3A1, BTN3A1 expression was investigated by flow cytometry in CD14+ cells, DC<sup>THP1</sup>, DC<sup>U937</sup>, and DC without detecting any difference under baseline conditions or after ZA treatment (Supplementary Fig. 2D). BTN3A1 and ABCA1 were co-immunoprecipitated in DC<sup>U937</sup> and DC, which were the only cells to express detectable amounts of ABCA1 (Fig. 5a). ZA treatment increased ABCA1 expression but did not modify BTN3A1 expression. The physical interaction between ABCA1 and BTN3A1 was confirmed in DC<sup>U937</sup> and DC by the proximity

ligation assay (PLA) (Fig. 5b). Next, we tested the presence of interactions between apoA-I and ABCA1 or BTN3A1. After crosslinking of apoA-I to cell surface proteins and immunoprecipitation with anti-apoA-I antibody, we found that apoA-I and ABCA1 are physically associated as previously reported<sup>20</sup>, whereas no interaction was detected between apoA-I and BTN3A1 (Fig. 5c).

To determine the reciprocal contributions to extracellular IPP release, BTN3A1 and ABCA1 were alternatively or concurrently silenced in untreated and ZA-treated DC. The efficacy and specificity of siRNA are shown in Fig. 5d: untreated DC (ZA-) expressed detectable levels of ABCA1, which further increased in ZA-treated DC (ZA+) and disappeared in untreated and ZA-treated *Abca1*-silenced and *Abca1*+*Btn3a1*-silenced DC, whereas ABCA1 expression was not suppressed in *Btn3a1*-silenced DC. To determine whether IPP was physically associated with ABCA1, DC were treated as shown in Fig. 5d, radiolabelled with  $1\ \mu\text{M}$  [<sup>14</sup>C]-IPP, and chemically crosslinked after extensive washing. ABCA1 was immunoprecipitated by plasma-membrane extracts, resolved by sodium dodecyl sulfate-

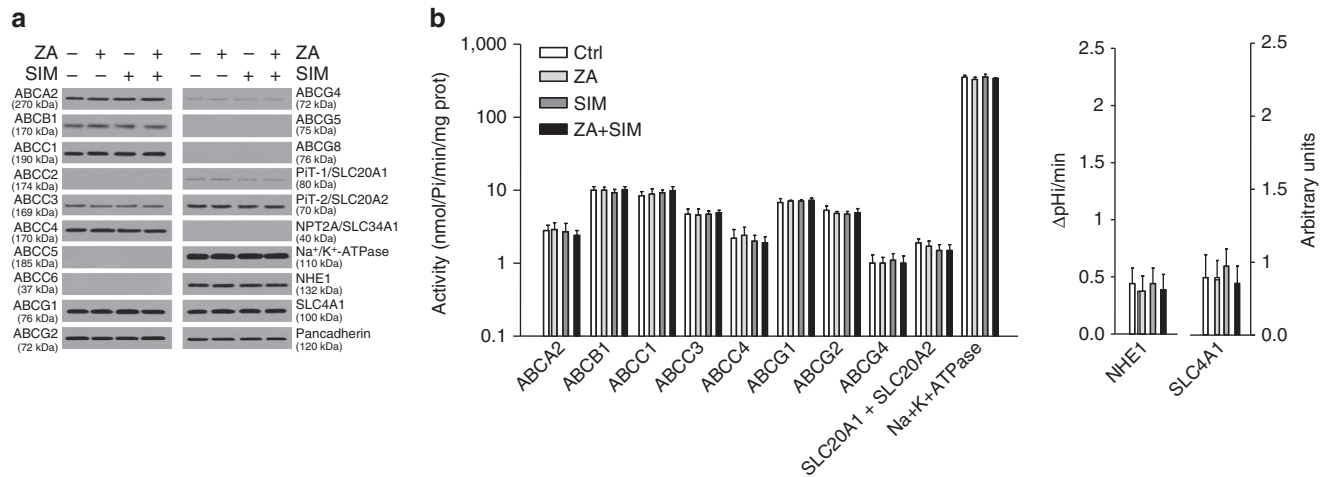


**Figure 3 | ZA treatment does not affect other transporters in ZA and SIM-treated DC.** Levels of the indicated plasma-membrane-associated proteins are evaluated by western blotting in biotinylated extracts from untreated or 1  $\mu$ M ZA and/or simvastatin (SIM) treated DC. Pancadherin is employed as a control of equal protein loading. The blots are representative of one out of the three experiments. **(b)** Activities of the indicated plasma-membrane-associated proteins are measured after immunopurification from the biotinylated extracts of DC treated, as shown in **a**. The results are expressed as nmoles hydrolysed phosphate (Pi)/min/mg proteins according to the previously prepared titration curve. The NHE1 activities and SLC4A1 activities are fluorimetrically measured, and the results are expressed as  $\Delta$ pHi/min and arbitrary units, respectively. The bars represent the mean  $\pm$  s.e.m. of three experiments. None of the differences is statistically significant.

polyacrylamide gel electrophoresis (SDS-PAGE) and probed with an anti-ABCA1 antibody that recognizes the N-terminal extracellular loop (Fig. 5e, left) or subjected to autoradiography (Fig. 5e, right). As internal control, biotinylated plasma-membrane extracts from ZA-treated DC were subjected to limited digestion to obtain distinct extracellular and intracellular ABCA1 fragments<sup>21,22</sup>. Autoradiography showed a positive signal in untreated DC coincidental with the expected ABCA1 molecular weight, which was increased in ZA-treated DC. The radioactive signal was still present in *Btn3a1*-silenced DC, whereas it was not detectable in *Abca1*-silenced and *Abca1/Btn3a1*-silenced DC. In dithiothreitol + trypsin-treated DC, the radioactive signal was coincidental with the 100 kDa band and, to a lesser extent, with the 150 kDa band, which suggests that IPP is physically associated with the N-terminal extracellular domain of ABCA1.

The functional consequences of *Abca1*-silencing and *Btn3a1*-silencing are shown in Fig. 5f,g. Minimal variations of extracellular IPP levels were induced when *Abca1* and/or *Btn3a1* were silenced in the absence of ZA-treatment (Fig. 5f). Conversely, ZA-treated *Abca1*-silenced DC showed a significant reduction in the ability to release extracellular IPP, whereas ZA-treated *Btn3A1*-silenced DC were only marginally affected. When both genes were silenced, further reduction in extracellular IPP release was observed (Fig. 5f). As expected, V $\gamma$ 9V $\delta$ 2 T cell proliferation induced by supernatants from *Abca1*- and/or *Btn3A1*-silenced ZA-treated DC matched the extracellular IPP concentrations (Fig. 5g). These data indicate that ABCA1 plays a major role in extracellular IPP release; this function is facilitated by physical interactions with IPP, apoA-I and BTN3A1.

**ZA increases IPP efflux via LXR $\alpha$ -mediated *Abca1* activation.** Simvastatin inhibits the mevalonate pathway upstream to FPPS<sup>3</sup>. As expected, simvastatin decreased extracellular IPP release in both untreated and ZA-treated DC (Fig. 6a). Interestingly, simvastatin also reduced ABCA1 (Fig. 6b) and apoA-I expression (Fig. 6c). These data confirm the close relationship

between the mevalonate pathway, ABCA1, apoA-I and extracellular IPP release.

ABCA1 and apoA-I expressions are controlled by the liver X receptor (LXR)/retinoic acid X receptor (RXR) transcription factor receptor family<sup>23,24</sup>. We investigated whether ZA and simvastatin regulated ABCA1 and apoA-I expression via these transcription factors. Untreated DC expressed both LXR $\alpha/\beta$  and RXR in nuclear extracts (Fig. 6d). ZA treatment increased LXR $\alpha$  protein levels, whereas LXR $\beta$  and RXR intracellular distribution was unaffected (Fig. 6d). LXR $\alpha$  bound to *Abca1* and *apoA-I* promoters was increased (Fig. 6e), leading to increased *Abca1* and *apoA-I* mRNA levels (Fig. 6f). These ZA-induced effects were neutralized by simvastatin (Fig. 6d–f). These data indicate that ZA-induced LXR $\alpha$  activity is crucial to increase ABCA1 and apoA-I expression in DC and promotes extracellular IPP release.

To reinforce the role of LXR $\alpha$ , the experiments mentioned above were repeated using THP-1 cells, which are unable to release extracellular IPP, even after DC differentiation and ZA treatment. Unlike DC, LXR $\alpha$  and LXR $\beta$  failed to translocate into the nucleus after ZA treatment in THP-1 cells and DC<sup>THP1</sup> (Supplementary Fig. 4A). As expected, *Abca1* and *apoA-I* mRNA levels remained unchanged by ZA treatment (Supplementary Fig. 4B). These data confirm that LXR $\alpha$  is critical to induce *Abca1* and *apoA-I* transcription and protein expression after ZA-induced IPP accumulation.

To determine whether ZA or IPP was responsible for LXR $\alpha$  activation, genomic DNA was extracted from DC and challenged with increasing ZA and IPP concentrations in the presence of the human recombinant LXR $\alpha$  transcription protein. Only IPP was able to induce a dose-dependent LXR $\alpha$  binding to the LXR responsive element (LRE) in the *Abca1* promoter (Fig. 6g). Optimal LXR $\alpha$  activation was induced by 500 pM IPP, which falls in the range of concentrations detected in the supernatants of ZA-treated DC (Fig. 6g). We tested whether other isoprenoids generated in the mevalonate pathway, such as FPP and GGPP, can also induce LXR $\alpha$  activation and we found that the former had no effect, whereas the latter downregulated LXR $\alpha$  activation (Supplementary Fig. 5) as previously reported<sup>25</sup>.

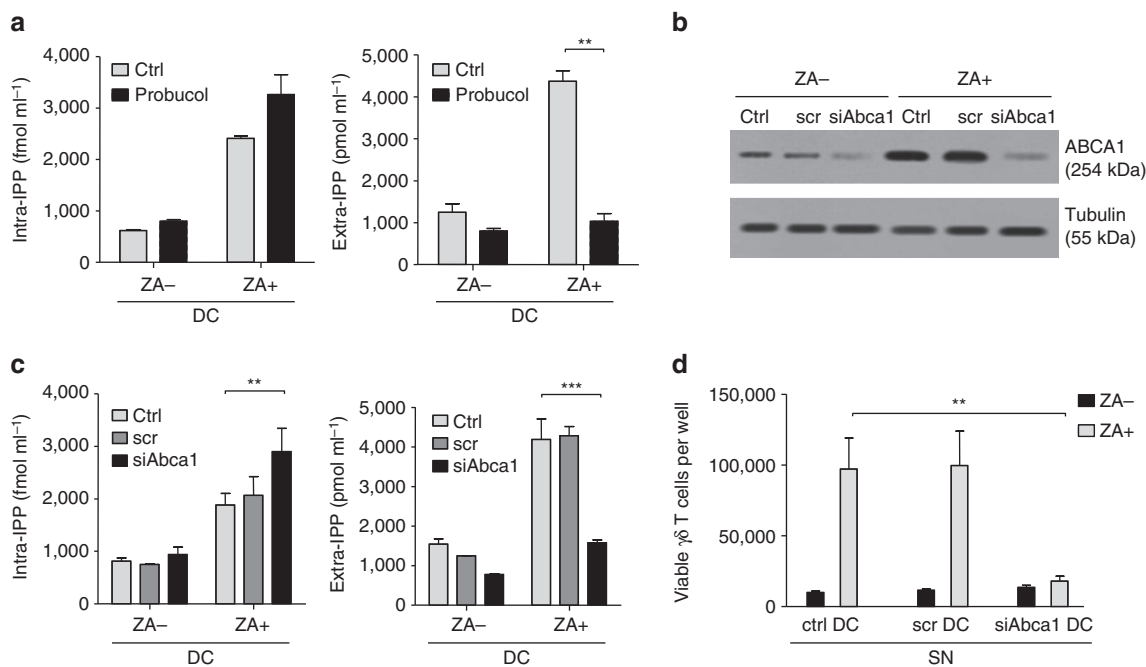


**Figure 4 | ABCA1 has a pivotal function in extracellular IPP release.** (a) Intracellular and extracellular IPP levels generated by untreated (ZA-) and ZA-treated (ZA+) DC incubated for 24 h in fresh medium (CTRL) or with 10  $\mu$ M probucol to inhibit ABCA1 function. Probucol marginally increased intracellular IPP but significantly decreased extracellular IPP release in ZA-treated DC (\*\* $P < 0.01$ ; ANOVA). The bars represent the mean  $\pm$  s.e.m. of four experiments. (b) Western blot analysis of ABCA1 expression in untreated (ZA-) and ZA-treated (ZA+) DC after *Abca1*-silencing with siRNA (scrambled [scr] non-targeting siRNA; siAbca1: *Abca1*-silencing siRNA). The blots are representative of one out of the three experiments.  $\beta$ -tubulin was employed as the control of equal protein loading. (c) Intracellular and extracellular IPP levels in DC incubated for 48 h in fresh medium (CTRL) or in the presence of scr or *Abca1*-silencing siRNA (siAbca1). ZA (1  $\mu$ M) was added in the last 24 h. Extracellular IPP release is significantly lower in *Abca1*-silenced ZA-treated DC. Bars represent the mean  $\pm$  s.e.m. of six experiments (\*\* $P < 0.01$ ; \*\*\* $P < 0.001$ ; ANOVA). (d) V $\gamma$ 9V $\delta$ 2 T cell proliferation after 7-day PBMC stimulation with supernatants from DC treated as reported in c. Supernatant from *Abca1*-silenced ZA-treated DC is unable to induce V $\gamma$ 9V $\delta$ 2 T cell proliferation (\*\* $P < 0.01$ ; Wilcoxon-Mann-Whitney). The bars represent the mean  $\pm$  s.e.m. of six experiments. ANOVA, analysis of variance.

Next, we investigated whether ZA and/or IPP also increased the enzyme activity of ABCA1 in addition to its expression. Identical aliquots of ABCA1 were immunopurified from the plasma membrane of DC and incubated with increasing concentrations of ZA (Supplementary Fig. 6A) or IPP (Supplementary Fig. 6B). The experimental conditions were established to enable any change in ATPase activity to be referred to differences in enzyme activity instead of protein expression. The results indicate that neither ZA nor IPP were able to directly upregulate ABCA1 ATPase-activity (Supplementary Fig. 6A,B). Next, we compared the ATPase activity of ABCA1 immunopurified from the plasma membrane of untreated and ZA-treated CD14+ cells and DC. Untreated CD14+ cells exhibited the lowest ATPase activity, which remained unaffected by ZA treatment, whereas untreated DC revealed intermediate values, which almost doubled in ZA-treated DC (Supplementary Fig. 6C). The results suggest that the increased ATPase activity in ZA-treated DC is more likely due to increased ABCA1 protein levels than to the direct effect exerted by ZA or IPP on its enzymatic activity.

#### PI3K/Akt/mTOR pathway regulates IPP release via LXR $\alpha$ /Abca1.

Akt suppresses cholesterol efflux by the activation of the mammalian target of rapamycin (mTOR) complex 1 TORC1, whereas the inhibition of mTORC1 by rapamycin promotes cholesterol efflux to apoA-I in an ABCA1-dependent manner<sup>26</sup>. The phosphoinositide 3-kinase (PI3K)/Akt/mTOR signalling pathway is also regulated by the Ras prenylation state, which is dependent on the mevalonate pathway in cancer cells and

activated T cells<sup>27,28</sup>. To investigate the involvement of the PI3K/Akt/mTOR signalling pathway in ABCA1/apoA-I-mediated extracellular IPP release, DC were incubated with specific PI3K (LY294002) and mTOR (rapamycin) inhibitors (refer to Methods and Supplementary Fig. 7 for technical details). Untreated DC showed detectable phosphorylation activity of both Akt and mTOR, which was very effectively blocked by ZA treatment. Akt and mTOR phosphorylation activities were fully recovered by simvastatin treatment in ZA-treated DC (Fig. 7a), although simvastatin also induces intracellular isoprenoid deprivation and Ras deprenylation<sup>29,30</sup>. A possible explanation is that isoprenoid deprivation recovers the activity of the PI3K/Akt/mTOR pathway via induction of the endoplasmic reticulum (ER) stress and unfolded protein responses (UPR), as previously reported<sup>31</sup>. In line with this hypothesis, we have demonstrated that several ER-stress-related genes are significantly upregulated in ZA + simvastatin-treated compared with untreated DC (Supplementary Data 1), as previously reported with ZA or simvastatin in other cell types<sup>32,33</sup>.

PI3K and mTOR inhibitors mimicked the effect of ZA by significantly increasing nuclear LXR $\alpha$  protein levels (Fig. 7b), LXR $\alpha$  transcriptional activity (Fig. 7c), and ABCA1 and apoA-I protein expression (Fig. 7d). Unlike ZA, LY294002 and rapamycin did not increase intracellular IPP levels as these inhibitors do not target the mevalonate pathway (Fig. 7e, left). However, both inhibitors increased extracellular IPP release as they upregulated ABCA1 and apoA-I protein expression. However, LY294002 and rapamycin did not achieve ZA-induced extracellular IPP values as they did not induce intracellular IPP accumulation (Fig. 7e, right).

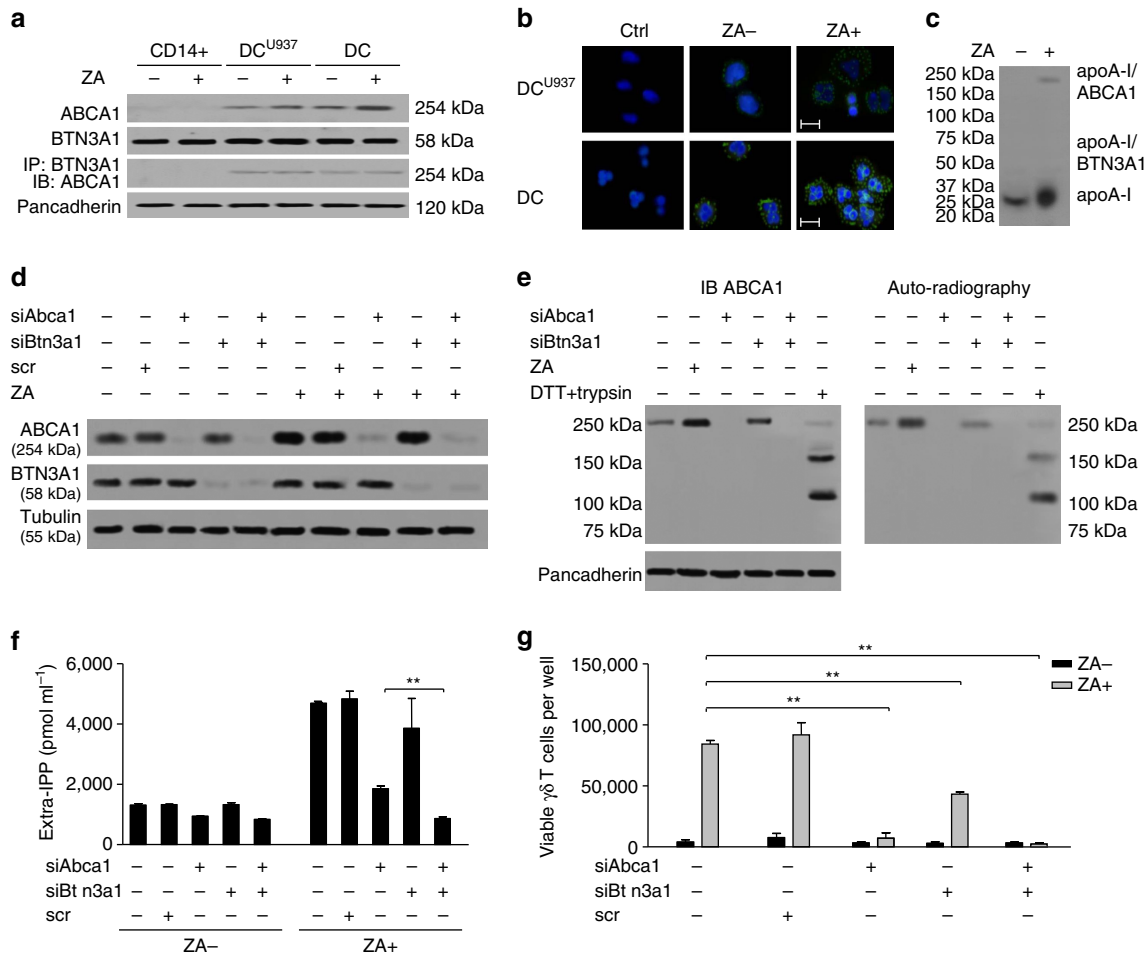


**Figure 5 | ABCA1 interactions with BTN3A1, apoA-I and IPP.** (a) ABCA1 and BTN3A1 co-immunoprecipitate in untreated and ZA-treated DC<sup>U937</sup> and DC but not in CD14+ cells, and ZA treatment does not modify BTN3A1 expression. Pancadherin is employed as a control of equal protein loading (one out of three blots). (b) PLA of ABCA1-BTN3A1 interaction by confocal laser-scanning microscopy (ocular lens: × 10; objective: × 63). Ctrl: cells without primary antibodies. Scale bar, 10 μm; blue: nuclear staining (DAPI); green: ABCA1/BTN3A1 interaction (one out of the three experiments). (c) apoA-I is physically associated with ABCA1, not with BTN3A1. The expected molecular weight of apoA-I, ABCA1/apoA-I and BTN3A1/apoA-I are shown (one out of the three experiments). (d) ABCA1 and BTN3A1 expression in DC after incubation with siRNA for *Abca1* (siAbca1), *Btn3a1* (siBtn3a1) or with scrambled non-targeting siRNA (scr). β-tubulin was employed as control of equal protein loading (n = 3). (e) IPP is physically associated with ABCA1 in untreated and ZA-treated DC. The two bands of 150 and 100 kDa in the dithiothreitol (DTT)- and trypsin-treated DC lane are detected with an antibody specific for the N-terminal extracellular loop of ABCA1 in immunoblotting (IB; left). Autoradiography signal of the IPP-ABCA1 interaction (right). Pancadherin is employed as a control of equal protein loading (one out of three experiments). (f) Extracellular IPP release in *Abca1*- and/or *Btn3a1*-silenced DC left untreated (ZA-) or after ZA treatment (ZA+). The bars represent the mean ± s.e.m. of three experiments (\*\*P < 0.001, Wilcoxon-Mann-Whitney). (g) Vγ9Vδ2 T cell proliferation after 7-day PBMC stimulation with supernatants from *Abca1*- and/or *Btn3a1*-silenced DC. The bars represent the mean ± s.e.m. of three experiments (\*\*P < 0.01; Wilcoxon-Mann-Whitney).

**Discussion**

In this study, we confirm that soluble IPP can induce Vγ9Vδ2 T cell activation<sup>3,34</sup> and demonstrate that the plasma-membrane-associated transporter ABCA1 plays a major role in the extracellular IPP release from ZA-treated DC and other cells. apoA-I and BTN3A1 are also important contributors to this process, which ultimately causes the activation of Vγ9Vδ2 T cells. Although other metabolites downstream to IPP can also activate Vγ9Vδ2 T cells (that is, DMAPP, GPP, FPP and GGPP)<sup>35</sup>, none of these molecules achieved mitogenic concentrations in untreated DC and their levels further decreased after ZA treatment. These data exclude a contribution of these molecules in ZA-induced Vγ9Vδ2 T cell activation.

Cells that are unable to release extracellular IPP in baseline conditions or after ZA-induced intracellular IPP accumulation do not express ABCA1; contrariwise, cells with a high capacity to

release intracellular IPP express ABCA1 and further up-regulate its expression after ZA treatment. IPP is physically associated with the N-terminal extracellular domain of ABCA1 and this association is strengthened in ZA-treated cells that have increased intracellular ABCA1 and IPP levels.

ABCA1 upregulation by ZA treatment is associated with an increased apoA-I concentration in the supernatants. The mutual interaction between ABCA1 and apoA-I was confirmed by the ability of exogenously added apoA-I to facilitate extracellular IPP release, but only in cells that already express ABCA1 in baseline conditions or after ZA treatment. We cannot exclude *a priori* that other transporters are involved in IPP efflux. However, the unique relationship between ABCA1 upregulation and intracellular IPP accumulation was corroborated by the observation that ZA and simvastatin treatment, which increase IPP and decrease IPP respectively, do

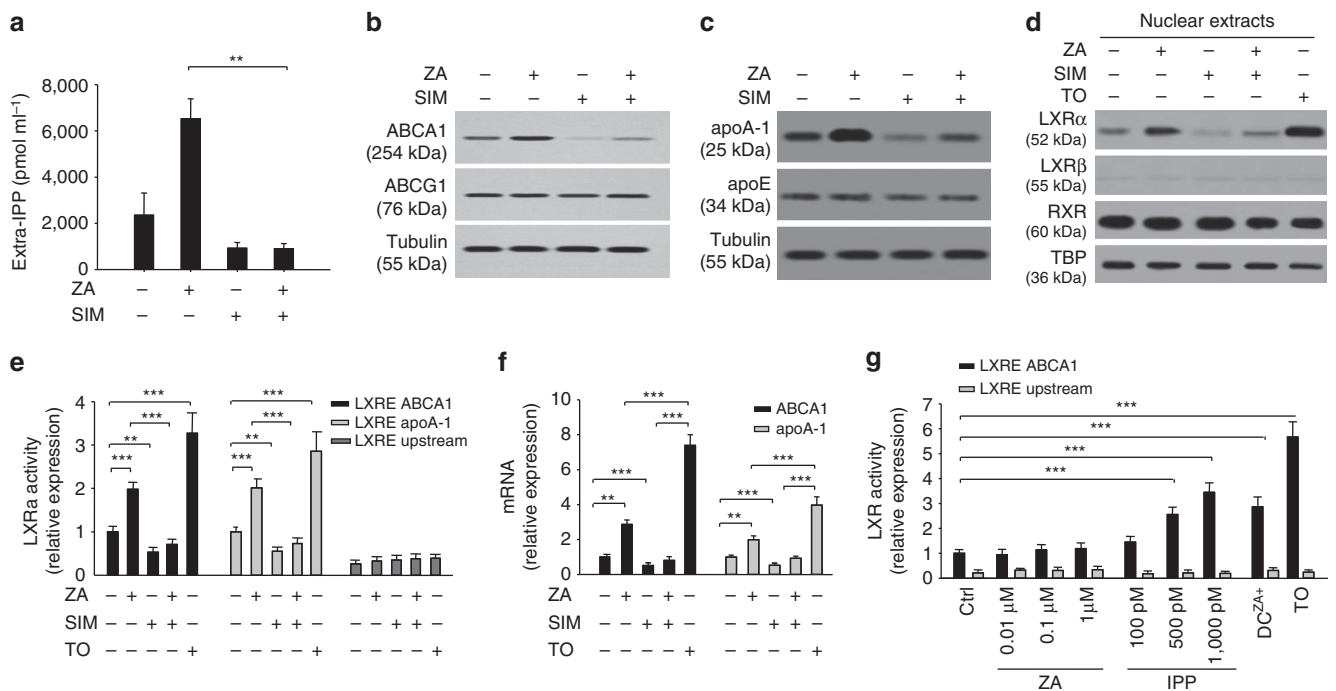


**Figure 6 | Regulation of ABCA1 and apoA-I expression via LXR $\alpha$  nuclear translocation.** (a) Extracellular IPP release in DC left untreated or incubated with 1  $\mu$ M ZA and/or simvastatin (SIM, 1  $\mu$ M). Simvastatin abrogated ZA-induced extracellular IPP release. Bars represent the mean  $\pm$  s.e.m. of four experiments (\*\* $P$  < 0.01; ANOVA). (b) ABCA1 expression in experimental conditions as in a. ZA increased ABCA1 expression, whereas simvastatin showed the opposite effect and abrogated ZA-induced ABCA1 upregulation. (c) apoA-I expression in experimental conditions, as shown in a. ZA increased apoA-I expression, whereas simvastatin exhibited the opposite effect and abrogated ZA-induced apoA-I upregulation. apoE was unaffected by ZA and/or simvastatin treatments. (d) LXR $\alpha$ , LXR $\beta$  and RXR levels were measured in nuclear extracts from DC incubated in the absence (–) or presence (+) of ZA and/or simvastatin. The LXR $\alpha$  activator TO-901317 (TO, 100 nM for 24 h) was employed as a positive control. ZA increased LXR $\alpha$  protein levels and this effect was antagonized by SIM. LXR $\beta$  and RXR were unaffected by ZA and/or simvastatin treatment.  $\beta$ -tubulin and TBP are employed as controls of equal protein loading as indicated. The blots are representative of one out of three experiments (b–d). (e) Activity of *Abca1* and *apoA-I* promoters, as shown in d. ZA increased and antagonized the ZA-induced LXR $\alpha$  transcriptional activity of *Abca1* and *apoA-I* promoters. The bars represent the mean  $\pm$  s.e.m. of three experiments (\*\* $P$  < 0.01; \*\*\* $P$  < 0.001; ANOVA). (f) *Abca1* and *apoA-I* mRNA levels in the experimental conditions, as shown in d. ZA increased the *Abca1* and *apoA-I* mRNA levels, whereas simvastatin had the opposite effect and antagonized ZA-induced upregulation. The bars represent the mean  $\pm$  s.e.m. of three experiments (\*\* $P$  < 0.01; \*\*\* $P$  < 0.001; ANOVA). (g) Evaluation of LXR $\alpha$  binding to LRE in the *Abca1* promoter. ZA did not modify LXR $\alpha$  transcriptional activity, whereas IPP induced a dose-dependent upregulation of LXR $\alpha$ -dependent *Abca1* transcription. LXR $\alpha$  transcriptional activity in ZA-treated DC and TO-induced LXR $\alpha$  transcriptional activity are reported as positive internal controls. The bars represent the mean  $\pm$  s.e.m. of four experiments (\* $P$  < 0.001; ANOVA). ANOVA, analysis of variance.

not modify the expression of other ABC transporters, phosphate transporters or other ubiquitous and unrelated pumps or channels. These results also eliminated the possibility that ABCA1 expression is upregulated merely because the cholesterol content of plasma membranes or the intracellular concentration of other mevalonate pathway-related metabolites are modified by ZA or simvastatin.

The experiments in which ABCA1 was functionally inhibited with probucol, or protein expression specifically silenced with siRNA, provided direct evidence that ABCA1 plays a major role in extracellular IPP release. Both treatments only slightly increased intracellular IPP concentrations in untreated and ZA-treated DC, probably because downstream enzymes in the mevalonate pathway like IPP isomerase and prenyl transferases intervene to handle IPP accumulation in the absence of ABCA1 upregulation. More importantly, probucol and *Abca1*-silencing abrogated extracellular IPP release. IPP deprivation in the supernatants from ABCA1-inhibited DC was functionally confirmed by the inability to induce V $\gamma$ 9V $\delta$ 2 T cell proliferation.

BTN3A1 is also involved in extracellular IPP release. BTN3A1 is an immunoglobulin superfamily protein playing a key role in V $\gamma$ 9V $\delta$ 2 T cell activation and target recognition by V $\gamma$ 9V $\delta$ 2 T cells<sup>4,6,7,36–39</sup>. The allosteric/sensor model anticipates that

intracellular interactions between the phosphoantigen domain and the B30.2 domain of BTN3A1 induce conformational changes of the transmembrane domain that are sensed by V $\gamma$ 9V $\delta$ 2 T cells, which cause their activation. The presentation model predicts that BTN3A1 functions as an antigen-presenting molecule for V $\gamma$ 9V $\delta$ 2 T cells by extracellularly binding phosphoantigens<sup>7</sup>. The two models are not mutually exclusive and both models contemplate the possible contribution of a second protein that has yet to be characterized<sup>14,40</sup>. In the allosteric/sensor model, the unknown protein is expected to facilitate intracellular interactions between phosphoantigens and the B30.2 domain, whereas the unknown protein in the presentation model is expected to facilitate the release of endogenous phosphoantigens and the subsequent binding to extracellular BTN3A1. It has been proposed that this hypothetical transporter only intervenes when intracellular IPP exceeds a critical threshold<sup>40</sup>. Our results unveils a new function of BTN3A1 by showing its contribution to extracellular IPP release in cooperation with ABCA1 and apoA-I. BTN3A1 is physically associated with ABCA1 but is not associated with apoA-I. BTN3A1 expression is not required to maintain the association between ABCA1 and IPP; it is not correlated with intracellular IPP concentrations and/or extracellular IPP



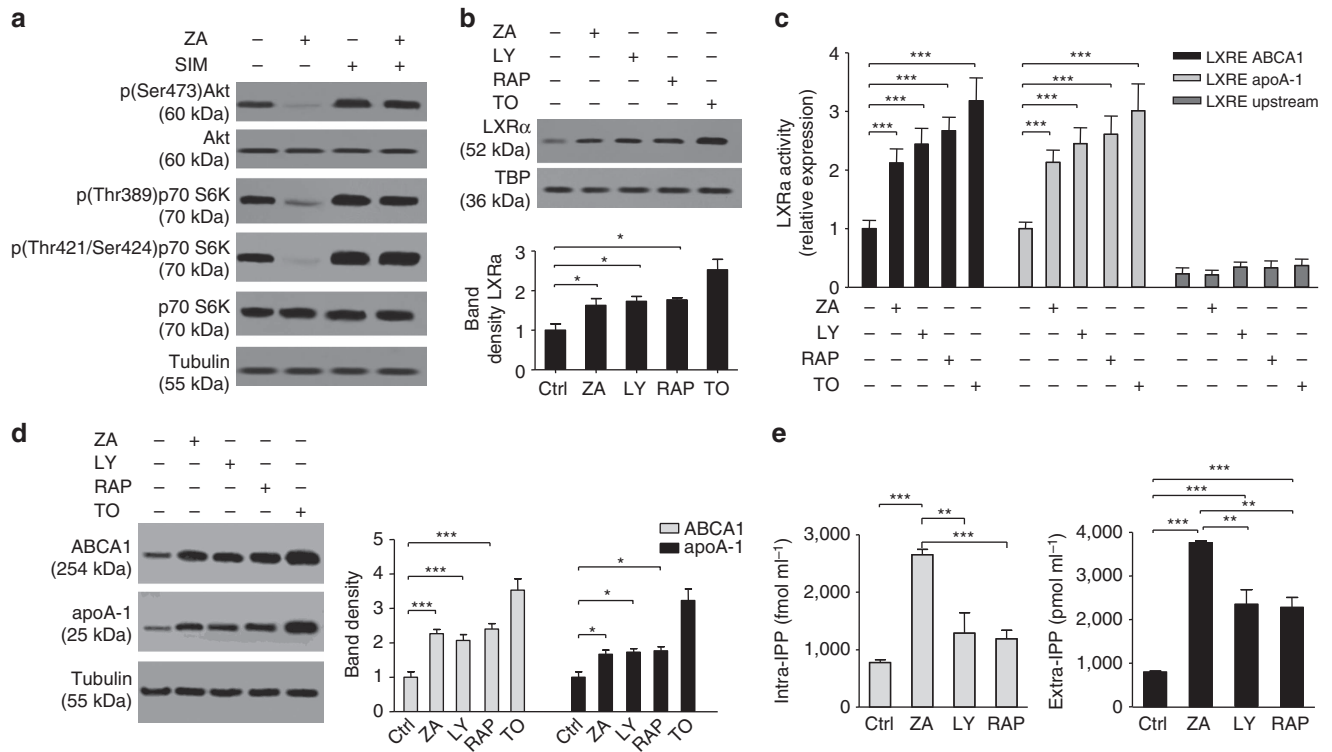


**Figure 7 | The PI3K/Akt/mTOR pathway regulates IPP release via LXR $\alpha$ /Abca1 activation.** (a) Targeting the Mev pathway fine-tunes the PI3K/Akt/mTOR signalling pathway. DC were left untreated or incubated with 1  $\mu$ M ZA or simvastatin (SIM). ZA decreased, whereas simvastatin increased the signalling activity of the PI3K/Akt/mTOR pathway. (b) DC were grown for 24 h in the absence (-) or presence (+) of ZA (1  $\mu$ M), the PI3K inhibitor LY294002 (LY, 200  $\mu$ M for 24 h), the mTOR inhibitor rapamycin (RAP, 20 nM for 24 h). The LXR $\alpha$  activator TO-901317 (TO, 100 nM for 24 h) was included as positive control. PI3K/mTOR inhibitors increased LXR $\alpha$  nuclear translocation, such as ZA. Pooled data are obtained by densitometric analysis with ImageJ software (<http://imagej.nih.gov/ij/>). The results are expressed as arbitrary units ( $n=3$ ) (\* $P<0.05$ ; ANOVA). (c) Evaluation of LXR $\alpha$  binding to LRE sequences in the *Abca1* and *apoA-1* promoters by ChIP assay. ZA, LY294002 and rapamycin increased *Abca1* and *apoA-1* promoters activity. The bars represent the mean  $\pm$  s.e.m. of three experiments (\*\*\* $P<0.001$ ; ANOVA). (d) Western blot analysis of ABCA1 and apoA-1 expression in experimental conditions, as shown in b. PI3K and mTOR inhibition mimicked ZA treatment and upregulated ABCA1 and apoA-1 expression.  $\beta$ -tubulin and TBP were employed as a control of equal protein loading, as indicated. All blots are representative of out the of three experiments. Pooled data are obtained by densitometric analysis with ImageJ software (<http://imagej.nih.gov/ij/>). The results are expressed as arbitrary units ( $n=3$ ). (\* $P<0.05$ , \*\*\* $P<0.001$ ; ANOVA). (e) Intracellular and extracellular IPP levels in DC after incubation in experimental conditions, as shown in b. As expected, PI3K/Akt/mTOR inhibition only increased extracellular IPP. The bars represent the mean  $\pm$  s.e.m. of three experiments (\*\* $P<0.01$ , \*\*\* $P<0.001$ ; ANOVA). ANOVA, analysis of variance.

release and is not affected by ZA treatment. *Btn3a1*-silenced ZA-treated DC are only marginally penalized in the ability to release extracellular IPP compared with *Abca1*-silenced or *Btn3a1/Abca1*-double silenced DC. Remarkably, ZA-treated THP-1 cells and DC<sup>THP1</sup> accumulate higher amounts of intracellular IPP than ZA-treated DC (approximately 1,500 versus 900 fmol ml<sup>-1</sup>). In the absence of ABCA1 and despite identical BTN3A1 expression, DC<sup>THP1</sup> fail to release extracellular IPP and activate V $\gamma$ 9V $\delta$ 2 T cells. These data indicate that ABCA1 serves a major role in extracellular IPP release from ZA-treated DC; this function is fine-tuned by one-to-one physical interactions of ABCA1 with IPP, apoA-1 and BTN3A1. The functional hierarchy of these molecules may be very different to drive V $\gamma$ 9V $\delta$ 2 T cell activation and target cell recognition once IPP has been released in the microenvironment. In the absence of ZA-treated cells, it is possible that IPP internalization in selected cell subsets and the subsequent interaction with the intracellular B30.2 domain of BTN3A1 play a more critical role than ABCA1 and apoA-I to induce V $\gamma$ 9V $\delta$ 2 T cell activation.

We have deciphered two mechanisms that underlie ZA-induced ABCA1 and apoA-1 upregulation. *In vitro* chromatin immunoprecipitation (ChIP) experiments indicated that IPP

induces a dose-dependent LXR $\alpha$  binding to the LRE of the *Abca1* promoter. The degree of DNA binding of purified LXR $\alpha$  incubated with 500 pM IPP was similar to the degree of DNA binding that was obtained in nuclear extracts of ZA-treated DC, the intracellular IPP levels of which range between 500 and 1,000 pM. Thus, the first mechanism is initiated by intracellular IPP accumulation due to ZA-induced FPPS inhibition, which causes LXR $\alpha$  activation, upregulation of *Abca1/apoA-1* transcription and increased ABCA1 and apoA-I protein expression. IPP-induced LXR $\alpha$  activation in our model was highly specific and cannot be reproduced with FPP or GGPP: the former had no effect, whereas GGPP downregulated LXR $\alpha$  activation as previously reported<sup>25</sup>. The antagonistic effect exerted by simvastatin confirmed the central role of IPP accumulation. By inhibiting HMGCR upstream to FPPS, simvastatin prevents ZA-induced intracellular IPP accumulation, ABCA1 and apoA-I upregulation, extracellular IPP release and V $\gamma$ 9V $\delta$ 2 T cell activation. Unlike LXR $\alpha$ , DC express very low levels of LXR $\beta$ <sup>41</sup>, which remains unmodulated by ZA or simvastatin. Thus, the LXR $\alpha$ /LXR $\beta$  nuclear ratio is critical to fine-tune not only intracellular cholesterol concentrations in resting and activated conventional T cells to satisfy their metabolic requirements<sup>27</sup> but

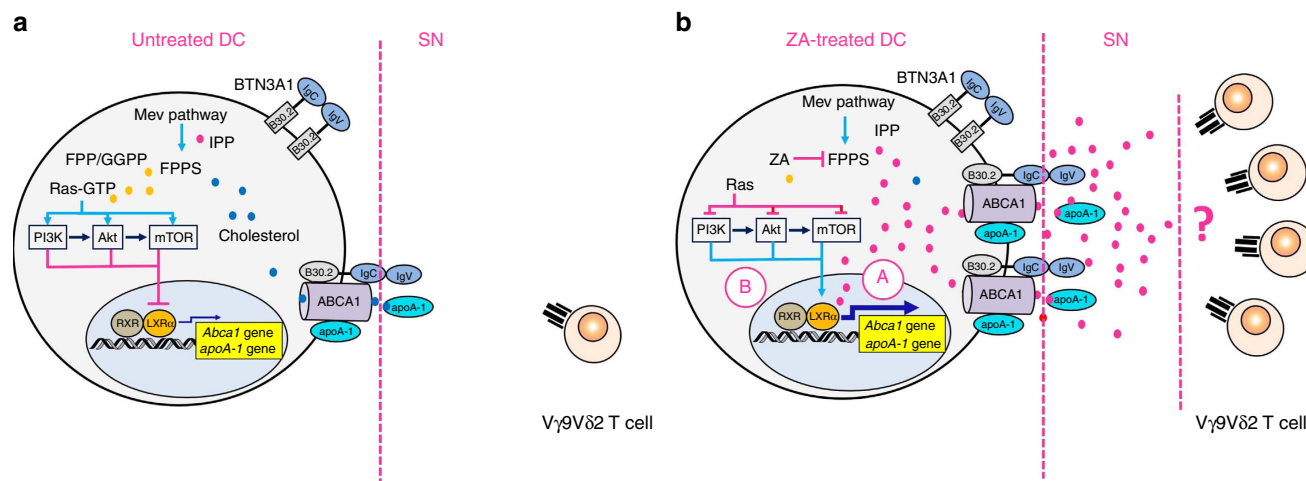


**Figure 8 | Mechanisms involved in IPP release from untreated and ZA-treated DC.** (a): Mevalonate (Mev) pathway of untreated DC generates isoprenoids (IPP: red circles; FPP/GGPP: yellow circles) and cholesterol (blue circles). Ras is prenylated in untreated DC (Ras-GTP) and causes the activation of the PI3K/Akt/mTOR signalling pathway and suppression of LXR $\alpha$  transcriptional activity. ABCA1 and apoA-I expression is finalized to tune the intracellular concentrations of cholesterol and other mevalonate pathway metabolites that were generated in physiological conditions. The supernatant obtained from untreated DC is unable to induce the proliferation of V $\gamma$ 9V $\delta$ 2 T cells as extracellular IPP concentrations are below a critical threshold. (b) Farnesyl pyrophosphate synthase (FPPS) is inhibited in ZA-treated DC, which causes intracellular IPP accumulation (red circles), and isoprenoid (yellow circles) and cholesterol (blue circles) deprivation. Intracellular IPP induces LXR $\alpha$  nuclear translocation (a), which enhances *Abca1* and *apoA-1* gene transcription and upregulation of ABCA1 and apoA-I expression. Isoprenoid deprivation concurrently causes Ras deprenylation (Ras), which relieves the inhibition operated by the PI3K/Akt/mTOR pathway on LXR $\alpha$  nuclear translocation (b). Thus, two mechanisms are operative in ZA-treated DC, which causes upregulation of ABCA1 and apoA-I expression and extracellular IPP and apoA-I release. The supernatant from ZA-treated DC contains sufficient amounts of IPP and apoA-I to induce the activation of V $\gamma$ 9V $\delta$ 2 T cells. The question mark in the right panel indicates that the mechanisms by which soluble IPP released in the supernatant from ZA-treated DC induces V $\gamma$ 9V $\delta$ 2 T cell activation remain to be elucidated.

also to regulate extracellular IPP release in DC and the subsequent activation of V $\gamma$ 9V $\delta$ 2 T cells. It is also possible that phosphoantigens are internalized from the microenvironment via fluid phase endocytosis or energy-dependent mechanism<sup>42</sup>, especially when extracellular concentrations are much higher than intracellular concentrations, as in the supernatants from ZA-treated cells after removal of these cells. In this case, LXR $\alpha$  activation, ABCA1, and apoA-I upregulation may be regulated by internalization of extracellular IPP.

The second mechanism is dependent on ZA-induced inhibition of the PI3K/Akt/mTOR signalling pathway<sup>26,30,43</sup>. This mechanism has been described in tumour cells and associated with anti-tumour ZA activity<sup>32,44</sup>. LXR $\alpha$  is also regulated by the PI3K/Akt/mTOR pathway with different outcomes according to the cell type<sup>26,45</sup>. In DC, ZA-induced inhibition of the PI3K/Akt/mTOR signalling pathway increased LXR $\alpha$ -induced transcription of *Abca1* and *apoA-1*, which causes enhanced protein expression, increased extracellular IPP release and V $\gamma$ 9V $\delta$ 2 T cell activation. Similar results were obtained by targeting the PI3K/Akt/mTOR pathway with inhibitors other than ZA, which also upregulated ABCA1 and apoA-1. These inhibitors, however, caused inferior extracellular IPP release as they do not target the mevalonate pathway and do not induce intracellular IPP accumulation.

The mechanism beyond ZA-induced PI3K/Akt/mTOR inhibition is likely due to intracellular isoprenoid deprivation instead of IPP accumulation. ZA decreases GTP-bound Ras and downstream Ras-regulated signalling pathways<sup>29,30</sup>. As activity of the PI3K/Akt/mTOR pathway is upregulated by Ras, Ras deprenylation is expected to downregulate PI3K/Akt/mTOR signalling and increase LXR $\alpha$  activation<sup>28</sup>. Simvastatin also induces intracellular isoprenoid deprivation and Ras deprenylation, but it unexpectedly restored the activity of the PI3K/Akt/mTOR signalling in ZA-treated DC. A possible explanation is that the concurrent ZA and simvastatin treatments are so stressful to induce the expression

of ER-stress-related and UPR genes, which causes the recovery of PI3K/Akt/mTOR signalling<sup>31</sup>.

Our results indicate that ABCA1 serves a pivotal role in extracellular IPP release in cooperation with apoA-I and BTN3A1. ABCA1 is upregulated by ZA via LXR $\alpha$  transcriptional activation that is induced by intracellular IPP accumulation and inhibition of the PI3K/Akt/mTOR signalling pathway. The supernatants of ZA-treated DC contain sufficient IPP concentrations to induce V $\gamma$ 9V $\delta$ 2 T cell activation also in the absence of DC, but the manner in which soluble IPP engages V $\gamma$ 9V $\delta$ 2 T cells remains to be determined (see Fig. 8 for a schematic representation). Thus, V $\gamma$ 9V $\delta$ 2 T cell activation can be regulated not only with drugs that target the mevalonate pathway, such as ZA and simvastatin but also with drugs that target the PI3K/Akt/mTOR signalling pathway. Moreover, our data credit ABCA1 with a novel immune function that is linked to the activation of V $\gamma$ 9V $\delta$ 2 T cells and contributes new perspectives for understanding the relationship between lipid metabolism and immune functions.

## Methods

**Chemicals.** Plasticware for cell cultures was obtained from Falcon (Becton Dickinson, Mountain View, CA). ZA was a gift from Novartis (Basel, Switzerland). Simvastatin was purchased from Calbiochem (Billerica, MA). The electrophoresis reagents were obtained from Bio-Rad Laboratories (Hercules, CA). The protein content of cell lysates was assessed with the BCA kit from Sigma Chemical Co (St Louis, MO). If not specified, all other reagents were purchased from Sigma Chemical Co.

**Cells.** Peripheral blood samples were drawn from healthy blood donors; the samples were provided by the local Blood Bank (Fondazione Strumia). Peripheral blood and bone marrow samples from multiple myeloma patients and B-cell chronic lymphocytic leukaemia patients who carried mutated or unmutated immunoglobulin heavy-chain variable regions were collected after informed consent and approval by the local Institutional Review Board (Comitato Etico Interaziendale A.O.U. Città della Salute e della Scienza di Torino—A.O. Ordine Mauriziano—A.S.L. TO1) were received (DG 767/2015). After isolation on a Ficoll-

Hypaque density gradient, PBMC from healthy donors were kept unfractionated or processed to purify CD14<sup>+</sup> cells and generate different antigen-presenting cell (APC) preparations. When PBMC from chronic lymphocytic leukaemia patients contained less than 90% of CD19<sup>+</sup>/CD5<sup>+</sup> cells, cells were purified by negative selection using a magnetic bead-activated cell sorting with a B cell Isolation Kit II (Miltenyi Biotec, Bologna, Italy). Bone marrow mononuclear cells (BMMC) from multiple myeloma and chronic lymphocytic leukaemia patients were left unfractionated to generate BMSC or were processed to purify CD138<sup>+</sup> multiple myeloma cells. Control BMMC from healthy donors were purchased from Stem Cell Technology (Peschiera Borromeo, Italy) to generate control BMSC. SKMM1, which is a multiple myeloma cell line, THP-1 and U937 cells, which are two monocytic leukaemia cell lines, and A549 cells, which is a non-small cell lung cancer cell line, were provided by the ATCC (Manassas, VA). The standard culture medium was RPMI 1640 (Euroclone, Milano, Italy) or HAM F12 medium (Euroclone) for A549 cells, which contain 10% fetal calf serum (FCS) (Euroclone), 2 mM L-glutamine, 100 U ml<sup>-1</sup> penicillin, and 100 mg ml<sup>-1</sup> streptomycin. Commercial cell lines were authenticated by microsatellite analysis using the PowerPlex kit (Promega Corporation, Madison, WI; last authentication: December 2015). The cells were checked for *Mycoplasma spp.* contamination by PCR every 3 weeks, and the contaminated cells were discharged.

**Dendritic cell generation.** CD14<sup>+</sup> cells were purified using CD14 MicroBeads and LS columns (Miltenyi Biotec) and incubated for 24 h in 24-well plates at 1 × 10<sup>6</sup> per ml in the presence or absence of 1 μM ZA. DC were generated as previously reported<sup>3</sup>. Purified CD14<sup>+</sup> cells were cultured in a standard culture medium at 0.5–1.5 × 10<sup>6</sup> cells per ml that were supplemented with GM-CSF (1000 U ml<sup>-1</sup>) and IL-4 (500 U ml<sup>-1</sup>) in flat-bottomed 24-well plates for 24 h. After 24 h, DC were left untreated (ZA-) or treated for an additional 24 h with 1 μM ZA (ZA+). To clear supernatants from any residual ZA, the DC were washed after incubation with ZA and re-plated with fresh medium for an additional 24 and 48 h (washed DC). DC<sup>THP1</sup> and DC<sup>U937</sup> were generated with the same procedure as previously described from THP-1 and U937 cells. The DC phenotype was verified by cytofluorimetric analysis as follows.

In selected experiments, supernatants obtained from different cell cultures were collected and saved for a subsequent quantification of intracellular IPP and extracellular IPP levels and apoA-1 and apoE levels and to investigate their ability to induce autologous Vγ9Vδ2 T cell proliferation.

**Bone marrow stromal cells generation.** BMSC were generated by seeding 1 × 10<sup>6</sup> BMMC/well in 24-well plates in a DMEM medium that was supplemented with 10% FCS and replaced every 3 days with fresh medium. After 4 days, non-adherent cells were washed off and adherent cells—predominantly fibroblast-like cells—were grown in DMEM medium with 10% FCS until confluence (2–3 weeks). The BMSC phenotype was determined by cytofluorimetric analysis as follows.

**Immune-phenotyping.** Phenotypic characterization of DC, Vγ9Vδ2 T cells, myeloma cells and BMSC cells was performed with multicolour flow cytometry. The following anti-human monoclonal-antibody combinations were employed in the characterization: (a) Vγ9Vδ2 T cells: anti-TCR Vγ9 (clone B6, BD Pharmingen, dilution 1/50), anti-CD3 (clone BW264/56, Miltenyi Biotec, dilution 1/11); (b) DC: anti-CD80 (clone 2D10, Miltenyi Biotec, dilution 1/11), anti-CD86 (clone FM95, Miltenyi Biotec, dilution 1/11), anti-HLA-DR (clone AC122, Miltenyi Biotec, dilution 1/11); (c) myeloma cells: anti-CD138 (clone 44F9, Becton Dickinson, dilution 1/20); anti-CD38 (clone IB6, Becton Dickinson, dilution 1/20); and (d) BMSC cells: anti-CD44 (clone G44-26, Becton Dickinson, dilution 1/20), anti-CD105 (clone 266, Becton Dickinson, dilution 1/20), anti-CD11a (clone HI11, Becton Dickinson, dilution 1/20). Three- and four-colour flow cytometry were performed with the appropriate combinations of fluorescein isothiocyanate (FITC), r-phycoerythrin-(PE), Tricolour-(Tri), Peridinin Chlorophyll Protein Complex (PerCP) or allophycocyanin-(APC) conjugated antibodies, a FACScan cell sorter, and CELLQuest software (Becton Dickinson). Gating strategies are reported in the Supplementary Fig. 8.

**Vγ9Vδ2 T cell activation and proliferation.** PBMC were plated for 7 days at 10<sup>6</sup> cells per ml in 96-wells round-bottomed plates at 37 °C in a humidified atmosphere of 5% CO<sub>2</sub> in air in the presence of 10 IU ml<sup>-1</sup> IL-2 (Eurocetis, Milano, Italy) and 1 μM ZA (kindly provided by Novartis Pharma, Oroggio, Italy). The standard culture medium was RPMI 1640 (Eurobio, Les Ulis, France), containing 10% FCS (Mascia Brunelli, Milano, Italy), 2 mM L-glutamine (Eurobio, Les Ulis, France), 100 U ml<sup>-1</sup> penicillin (Eurobio, Les Ulis, France) and 100 mg ml<sup>-1</sup> streptomycin (Eurobio, Les Ulis, France)<sup>3</sup>. Total counts of viable Vγ9Vδ2 T cells on day 7 were evaluated by multiplying total counts of viable cells per well, identified with the trypan blue staining assay, by the percentage of Vγ9Vδ2 T cells identified by flow cytometry<sup>46</sup>.

**Quantification of intracellular and extracellular IPP.** After 24 h culture, 1 × 10<sup>6</sup> cell per ml were incubated for another 24 h with 1 μCi of [<sup>3</sup>H]acetate (3,600 mCi mmol<sup>-1</sup>; Amersham International, Piscataway, NJ) to measure the

intracellular IPP synthesis. 300 μl cells lysate or culture supernatant was diluted 1:2 into an ice-cold acetonitrile solution containing 100 mM NaVO<sub>4</sub> and 250 mM NaF, and centrifuged at 1,200g for 5 min at 4 °C. After lyophilization under vacuum, samples were resuspended in 20 μl dimethylhexylamine and separated by thin layer chromatography (TLC; LK6D Whatmann silica gel Merck, Darmstadt, Germany), using 1:1 solution of 50% methanol/0.8 M ammonium formate, pH 7.4, containing 2 mM dimethylhexylamine as running buffer. Gels were exposed to an iodine-saturated atmosphere for 2 h, and the spot that corresponds to IPP was quantified by liquid scintillation counting (UltimaGold; PerkinElmer, Waltham, MA). According to the titration curve, the results are expressed as fmoles ml<sup>-1</sup> for intracellular IPP or pmoles ml<sup>-1</sup> for extracellular IPP.

**Efflux of exogenous [<sup>14</sup>C]-IPP.** To measure the efflux of an exogenous pulse of IPP, 1 × 10<sup>6</sup> cell ml<sup>-1</sup> were labelled for 1 h with 0.02 μCi of [<sup>14</sup>C] IPP (50 mCi mmol<sup>-1</sup>; Amersham International), washed five times with PBS and left for 24 h in fresh medium. After this incubation time, supernatants were collected and underwent the same analytical process that was used to measure endogenously generated extracellular IPP. The amount of [<sup>14</sup>C]IPP that was present in the culture medium at t<sub>0</sub> is considered to be 100%; the amount of [<sup>14</sup>C]IPP that was measured after incubation is expressed as a percentage relative to the amount measured at t<sub>0</sub>.

**MALDI-TOF/MS analysis.** Fifty μl of the culture medium of 1 × 10<sup>6</sup> CD14<sup>+</sup> or DC were resolved by 12% SDS-PAGE, then stained using colloidal Coomassie brilliant blue (18% v-v ethanol, 15% w-v ammonium sulphate, 2% v-v phosphoric acid, 0.2% w/v Coomassie brilliant blue G-250). Gel slices from Coomassie-stained gels aligned to the recombinant human apoE or apoA-I, which were employed as standards, were excised and digested as previously described<sup>47</sup>. Gel slices were destained in 50% v-v acetonitrile in 5 mM ammonium bicarbonate, dried using pure acetonitrile and rehydrated for 45 min at 4 °C with digestion buffer that contains 10 ng μl<sup>-1</sup> trypsin in 5 mM ammonium bicarbonate. Digestion proceeded overnight at 37 °C. The mass spectrometry analysis of peptides was performed using a matrix-assisted laser desorption/ionization-time-of-flight/mass spectrometry device (MALDI micro MX; Waters, Milford, MA, USA) that was equipped with a delayed extraction unit that operated in reflectron mode. The peptide solution was prepared with equal volumes of saturated a-cyano-4-hydroxycinnamic acid solution in 40% v/v acetonitrile-0.1% v/v trifluoroacetic acid. The MALDI-TOF was calibrated with a mix of PEG (PEG 1000, 2000 and 3000 at a ratio of 1:2:2) and mass spectra were acquired in the positive-ion mode. Peak lists were generated by ProteinLynx Global Server 2.2.5 (Waters, Milford, MA, USA) using the following parameters: external calibration with lock mass using a mass of 2465.1989 Da for ACTH (adrenocorticotrophic hormone), background subtract type adaptive that combined all scans, and de-isotoping with a threshold of 1%. The 25 most intense masses were employed for database searches against the SWISSPROT database using the free search program MASCOT (<http://www.matrixscience.com>). The following parameters were employed in the searches: taxa Homo sapiens, trypsin digest, one missed cleavage by trypsin, methionine oxidation as variable modification and allowed maximum error of 100 p.p.m.

**Western blotting.** The cells were lysed in a MLB buffer (125 mM Tris-HCl, 750 mM NaCl, 1% v/v NP40, 10% v/v glycerol, 50 mM MgCl<sub>2</sub>, 5 mM EDTA, 25 mM NaF, 1 mM NaVO<sub>4</sub>, 10 μg ml<sup>-1</sup> leupeptin, 10 μg ml<sup>-1</sup> pepstatin, 10 μg ml<sup>-1</sup> aprotinin, 1 mM phenylmethylsulphonyl fluoride, pH 7.5), sonicated and centrifuged at 13,000g for 10 min at 4 °C. Plasma-membrane-associated proteins were isolated by the biotinylation method, using the Surface Protein Isolation Kit (Fisher Scientific Inc., Rockford, IL)<sup>48</sup>. Twenty microgram of proteins from cell lysates or biotinylated extracts were subjected to western blotting and probed with the following antibodies: anti-ABCA1 (HJI, Abcam, Cambridge, UK, dilution 1/500), anti-ABCA2 (ab91571, Abcam, dilution 1/250), anti-ABCB1 (C219, Novus Biologicals, Littleton, CO, dilution 1/250), anti-ABCC1 (IU2H10, Abcam, dilution 1/100), anti-ABCC2 (M2 III-6, Abcam, dilution 1/50), anti-ABCC3 (sc-5776, Santa Cruz Biotechnology Inc., Santa Cruz, CA, dilution 1/500), anti-ABCC4 (ab77184, Abcam, dilution 1/250), anti-ABCC5 (sc-5781, Santa Cruz Biotechnology Inc., dilution 1/500), anti-ABCC6 (ab54826, Abcam, dilution 1/500), anti-ABCG1 (sc-11150, Santa Cruz Biotechnology Inc., dilution 1/1,000), anti-ABCG2 (sc-25882, Santa Cruz Biotechnology Inc., dilution 1/100), anti-ABCG4 (ab101528, Abcam, dilution 1/250), anti-ABCG5 (EPR6203, Abcam, dilution 1/500), anti-ABCG8 (ab126493, Abcam, dilution 1/500), anti-SR-BI (NB400-104, Novus Biologicals, dilution 1/1,000), anti-BTN3A1 (25221-1-AP, Proteintech, Chicago, IL, dilution 1/500), anti-apoA-I (SAB1104904, Sigma Chemical Co., dilution 1/1,000), anti-apoE (AV54283, Sigma Chemical Co., dilution 1/1,000), anti-PIT-1/SLC20A1 (ab58181, Abcam, dilution 1/200), anti-PIT-2/SLC20A2 (ab155259, Abcam, dilution 1/200), anti-NPT2A/SLC34A1 (ab151129, Abcam, dilution 1/500), anti-Na<sup>+</sup>/K<sup>+</sup>-ATPase (M7-PB-E9, Sigma Chemical Co., dilution 1/2,000), anti-Na<sup>+</sup>/H<sup>+</sup> exchanger 1/NHE1 (sc-136239, Santa Cruz Biotechnology Inc., dilution 1/500), anti-Cl<sup>-</sup>/HCO<sub>3</sub><sup>-</sup> transporter/SLC4A1 (EPR1426, Abcam, dilution 1/1,000), anti-phospho(Ser473)Akt (6F5, Millipore, Billerica, MA, dilution 1/1,000), anti-Akt (SKB1, Millipore, dilution 1/500), anti-phospho(Thr389)-p70 S6K (#9205, Cell Signalling

Technology, Danvers, MA, dilution 1/1,000), anti-phospho(Thr421/Ser424)-p70 S6K (#9204, Cell Signalling Technology, dilution 1/1,000), and anti-p70 S6K (#9202, Cell Signalling Technology, dilution 1/1,000). Anti- $\beta$ -tubulin (sc-5274, Santa Cruz Biotechnology Inc., dilution 1/1,000) and anti-pancaderhin (sc-1499, Santa Cruz Biotechnology Inc., dilution 1/500) were employed as a control of equal protein loading in whole cell and plasma-membrane extracts, followed by a peroxidase-conjugated secondary antibody. The proteins were detected by enhanced chemiluminescence (Bio-Rad Laboratories).

In the co-immunoprecipitation assays, 100  $\mu$ g of proteins from biotinylated plasma-membrane extracts, which were prepared as previously described, were immunoprecipitated with the anti-BTN3A1 antibody, using the PureProteome protein A and protein G Magnetic Beads (Millipore). The immunoprecipitated proteins were separated by SDS-PAGE and probed with the anti-ABCA1 or apoA-I antibodies. An anti-pancaderhin antibody was employed as the control for equal plasma-membrane protein loading.

To evaluate LXR $\alpha$ , LXR $\beta$  and RXR nuclear translocations, nuclear extracts were prepared using the Nuclear Extract kit (Active Motif, La Hulpe, Belgium). Ten microgram of nuclear proteins were resolved by SDS-PAGE and probed with anti-LXR $\alpha$  (61175, Active Motif, dilution 1/500), anti-LXR $\beta$  (ABN65, Millipore, dilution 1/500), anti-RXR (ab24363, Abcam, dilution 1/2,000) antibodies or with an anti-TFIID/TATA box-binding protein (TBP) antibody (58C9, Santa Cruz Biotechnology Inc., dilution 1/250) as the equal protein loading control.

The images of uncropped gels reported in main figures and Supplementary Figures are shown in Supplementary Figs 9 and 10.

**Abca1 and Btn3a1 silencing.** Two  $\times 10^5$  DC were transfected with Accell Human siRNA ABCA1, Accell Human BTN3A1 siRNA or 19–25 nucleotide non-targeting scrambled siRNAs (from Thermo Scientific Open Biosystems, Waltham, MA) per the manufacturer's instructions. The efficacy of silencing was verified by western blotting, as previously described.

**Proximity ligation assay.** The presence of ABCA1-BTN3A1 interactions was assessed with the PLA method using the DuoLink In Situ kit (Sigma Chemical Co.) per the manufacturer's instructions. A total of  $1 \times 10^4$  cells were seeded on sterile coverglass, washed with PBS, fixed for 10 min at room temperature with 4% v/v paraformaldehyde, washed twice with PBS, and incubated 30 min at 37 °C in a humidified chamber with 40  $\mu$ l of the kit-provided Blocking solution. A mouse anti-human ABCA1 (HJI, Abcam) and rabbit anti-human BTN3A1 (HPA012565, Sigma Chemical Co.) antibodies were added at 1:50 final dilution. Samples were maintained at 4 °C overnight. Slides were washed once with the Wash buffer A for 5 min at room temperature, and incubated 1 h at 37 °C with the respective PLA probes diluted 1:5 into 40  $\mu$ l diluent antibody solution. Samples were washed twice with wash buffer A for 5 min at room temperature and incubated for 30 min at 37 °C with 40  $\mu$ l ligation solution diluted 1:5 into RNase/DNAse-free water and containing 25 mU ligase. After two washes at the rate of 2 min per each at room temperature, amplification was performed by adding 40  $\mu$ l amplification solution that was diluted 1:5 into RNase/DNAse-free water and contained 125 mU polymerase. Samples were maintained for 2 h at 37 °C, washed twice with undiluted wash buffer B for 10 min, once with wash buffer B, diluted 1:100 for 1 min, and mounted with the DuoLink In Situ Mounting medium, which contained 4',5'-diamidino-2 phenylindole dihydrochloride (DAPI) to counterstain cells' nuclei. Cells were examined using a Leica TCS SP2 AOP confocal laser-scanning microscope (Leica Microsystem, Wetzlar, Germany). A minimum of five fields were examined for each experimental condition.

**Crosslinking assay.** Crosslinking of apoA-I to cell surface proteins was performed as previously reported<sup>20</sup>. After labelling for 2 h at 37 °C with 5  $\mu$ g ml<sup>-1</sup> [<sup>125</sup>I]-apoA-I and chemically crosslinking with dithiobis(succinimidyl propionate) (DSP), cells were lysed and subjected to immunoprecipitation with an anti-apoA-I antibody (SAB1104904, Sigma Chemical Co., dilution 1/100). Samples were resolved by SDS-PAGE, and blotted proteins were detected by autoradiography (Kodak BioMax MR-1, PerkinElmer).

**IPP-ABCA1 interaction.** IPP-ABCA1 interaction was measured in the cells labelled with 1  $\mu$ M [<sup>14</sup>C]-IPP for 1 h. After extensively washing (five washing steps of 5 min with PBS) to remove any traces of residual [<sup>14</sup>C]-IPP in the extracellular medium, the cells were grown in fresh medium for 1 h and fixed with DSP. The surface proteins were isolated with the Surface Protein Isolation Kit (Fisher Scientific Inc. A total of 500  $\mu$ g of surface proteins were subjected to immunoprecipitation with an anti-ABCA1 antibody (HJI, Abcam, dilution 1/50). As an internal control, cells were incubated 5 min with 2 mM dithiothreitol, and the biotinylated extracts were subjected to limited digestion with 10  $\mu$ g ml<sup>-1</sup> trypsin, as reported<sup>21,22</sup>. Immunopurified ABCA1 was resolved by SDS-PAGE, and run in duplicate on the same gel. One part of the gel was probed with the anti-ABCA1 antibody; the second part was dried and subjected to autoradiography to visualize the [<sup>14</sup>C]-IPP signal.

**Quantitative real time-PCR and PCR array.** Total RNA was reverse-transcribed using the iScript cDNA Synthesis Kit (Bio-Rad Laboratories). The qRT-PCR was performed with the IQ SYBR Green Supermix (Bio-Rad). The same cDNA preparation was employed to quantify the genes of interest and the housekeeping gene *S14*. The primer sequences, which were designed using the qPrimerDepot database (<http://primerdepot.nci.nih.gov/>), were as follows: for *Abca1*: 5'-CAGAGCTCACAGCAGGGAC-3'; 5'-CTTCTCCGCAAGGCTTGTTC-3'; for *apoA-I*: 5'-CCCAGTGTCAAGGAGCTTT-3', 5'-TGGATGTGCTCAAAGACAGC-3'; for *S14*: 5'-CGAGGCTGATGACCTGTTCT-3'; 5'-GCCCTCTCCACTCTCTCTT-3'. The relative quantification was performed by comparing each PCR product with the housekeeping PCR product *S14*, using the Bio-Rad Software Gene Expression Quantitation (Bio-Rad). PCR arrays were generated using 1  $\mu$ g cDNA and Human Unfolded Protein Response Plus RT<sup>2</sup> Profiler PCR Array (Bio-Rad Laboratories) according to the manufacturer's instructions. Data analysis was performed using the PrimePCR Analysis Software (Bio-Rad Laboratories).

**Chromatin Immunoprecipitation.** ChIP samples were prepared as described by Campia *et al.*<sup>49</sup>, using a ChIP-tested anti-LXR $\alpha$  antibody (61175, Active Motif, dilution 1/50). The putative Liver X Receptor Response Element (LRE) sites on *Abca1* and *apoA-I* human promoters were validated with the MatInspector Software (<https://www.genomatix.de/matinspector.html>). Primer sequences were as follows: for *Abca1* promoter: 5'-GGAGGACAGGCTTGTACC-3'; 5'-CTCTCCGCAATTACGGG-3'; for *apoA-I* promoter: 5'-AACTGCCACACACTCCAT-3'; 5'-TCCTTCTGCAGTCTCTAAGCA-3'. Primers used as negative internal controls for a nonspecific 10 000 bp upstream sequence, were as follows: 5'-GTGGTGCTGAGGAAGAGAG-3' and 5'-GCAACAAGTAGGCACAA GCA-3'. The immunoprecipitated products were amplified by qRT-PCR.

In *in vitro* ChIP experiments, total DNA from  $1 \times 10^9$  DC was extracted using the GenElute Mammalian Genomic DNA Miniprep Kit (Sigma Chemical Co.), sonicated, incubated with 1 ng of recombinant human LXR $\alpha$  protein (Abcam), immunoprecipitated with the anti-LXR $\alpha$  antibody and processed as previously described.

**Activity of plasma-membrane-associated transporter and channels.** Plasma-membrane vesicles enriched for ATP-binding cassette transporters were prepared as detailed elsewhere with minor modifications<sup>50</sup>. Cells were washed with Ringer's solution (148.7 mM NaCl, 2.55 mM K<sub>2</sub>HPO<sub>4</sub>, 0.45 mM KH<sub>2</sub>PO<sub>4</sub>, 1.2 mM MgSO<sub>4</sub>; pH 7.4), lysed on crushed ice with lysis buffer (10 mM HEPES/Tris, 5 mM EDTA, 5 mM EGTA, 2 mM dithiothreitol; pH 7.4) supplemented with 2 mM phenylmethylsulfonyl fluoride, 1 mM aprotinin, 10  $\mu$ g ml<sup>-1</sup> pepstatin, 10  $\mu$ g ml<sup>-1</sup> leupeptin, and subjected to nitrogen cavitation at 1200 p.s.i for 20 min. Samples were centrifuged at 300g for 10 min, diluted 1:4 in the pre-centrifugation buffer (10 mM Tris/HCl, 25 mM sucrose; pH 7.5), overlaid on a sucrose cushion (10 mM Tris/HCl, 35% w/v sucrose, 1 mM EDTA; pH 7.5) and centrifuged at 14,000g for 10 min. The interface was collected, diluted 1:5 in the centrifugation buffer (10 mM Tris/HCl, 250 mM sucrose; pH 7.5) and subjected to a third centrifugation at 100,000  $\times$  g for 45 min. The vesicle pellet was resuspended in 0.5 ml centrifugation buffer and stored at -80 °C until the use, after the quantification of the protein content. Proteins were extracted by non-denaturing immunoprecipitation using the previously indicated antibodies. The ATPase activity of immunopurified ABCA1, ABCA2, ABCB1, ABCC1, ABCC3, ABCC4, ABCG1, ABCG2 and ABCG4 was measured with a spectrophotometric method<sup>51</sup>. Samples (containing 25  $\mu$ g protein) were incubated for 30 min at 37 °C with 50  $\mu$ l of the reaction mix (25 mM Tris/HCl, 3 mM ATP, 50 mM KCl, 2.5 mM MgSO<sub>4</sub>, 3 mM dithiothreitol, 0.5 mM EGTA, 2 mM ouabain, 3 mM NaN<sub>3</sub>; pH 7.0). In each set of experiments, a blank containing 0.5 mM Na<sub>2</sub>VO<sub>4</sub> was included<sup>52</sup>. The reaction was stopped by adding 0.2 ml ice-cold stopping buffer (0.2% w/v ammonium molybdate, 1.3% v/v H<sub>2</sub>SO<sub>4</sub>, 0.9% w/v SDS, 2.3% w/v trichloroacetic acid, 1% w/v ascorbic acid). After a 30 min incubation at room temperature, the absorbance of the phosphate hydrolyzed from ATP was measured at 620 nm, using a Packard EL340 microplate reader (Bio-Tek Instruments, Winooski, MA). The absorbance was converted into  $\mu$ mol hydrolyzed phosphate per min per mg proteins, according to the titration curve previously prepared. The activity of PiT-1/SLC20A1 and PiT-2/SLC20A2 (ref. 50), and Na<sup>+</sup>/K<sup>+</sup>-ATPase<sup>53</sup> were spectrophotometrically measured. The results are expressed as nmoles of hydrolysed phosphate per min per mg proteins according to the previously prepared titration curve. The NHE1 and SLC4A1 activities were fluorimetrically measured<sup>54,55</sup>, and the results are expressed as  $\Delta$ pHi/min and arbitrary units, respectively.

**Statistical analysis.** The results are expressed as the mean  $\pm$  s.e.m. Differences between the groups were evaluated with a one-way analysis of variance, a Wilcoxon-Mann-Whitney non-parametric test for paired or unpaired samples as appropriate and was considered to be statistically significant for *P* values < 0.05. Correlation analyses were performed with the non-parametric Spearman Rank Order test with a cutoff *P* value < 0.05. The GraphPad software was used for the statistical analyses; its symbology has been adopted to define the statistical significance (ns = *P* > 0.05; \**P* < 0.05; \*\**P* < 0.01; \*\*\**P* < 0.001; \*\*\*\**P* < 0.0001). The sample size was calculated

with the G\*Power software (www.gpower.hhu.de), with the setting  $P < 0.05$  as the significance level and 0.80 as the power of the study.

**Data availability.** The authors declare that all data supporting the findings of this study are available within the paper and its Supplementary Information files.

## References

- Gober, H. J. *et al.* Human T cell receptor gammadelta cells recognize endogenous mevalonate metabolites in tumor cells. *J. Exp. Med.* **197**, 163–168 (2003).
- Roelofs, A. J., Thompson, K., Gordon, S. & Rogers, M. J. Molecular mechanisms of action of bisphosphonates: current status. *Clin. Cancer Res.* **12**, 6222s–6230s (2006).
- Castella, B. *et al.* Immune modulation by zoledronic acid in human myeloma: an advantageous cross talk between  $V\gamma 9V\delta 2$  T cells,  $\alpha\beta$  CD8+ T cells, regulatory T cells, and dendritic cells. *J. Immunol.* **187**, 1578–1590 (2011).
- Harly, C., Peigné, C. M. & Scotet, E. Molecules and mechanisms implicated in the peculiar antigenic activation process of human  $V\gamma 9V\delta 2$  T Cells. *Front. Immunol.* **5**, 657 (2015).
- Fiore, F. *et al.* Enhanced ability of dendritic cells to stimulate innate and adaptive immunity on short-term incubation with zoledronic acid. *Blood* **110**, 921–927 (2007).
- Harly, C. *et al.* Key implication of CD277/butyrophilin-3 (BTN3A) in cellular stress sensing by a major human  $\gamma\delta$  T cell subset. *Blood* **120**, 2269–2279 (2012).
- Vavassori, S. *et al.* Butyrophilin 3A1 binds phosphorylated antigens and stimulates human  $\gamma\delta$  T cells. *Nat. Immunol.* **14**, 908–916 (2013).
- Gu, S., Nawrocka, W. & Adams, E. J. Sensing of pyrophosphate metabolites by  $V\gamma 9V\delta 2$  T Cells. *Front Immunol* **5**, 688 (2015).
- Palakodeti, A. *et al.* The molecular basis for modulation of human  $V\gamma 9V\delta 2$  T cell responses by CD277/butyrophilin-3 (BTN3A)-specific antibodies. *J. Biol. Chem.* **287**, 32780–32790 (2012).
- Vantourout, P. *et al.* Specific requirements for Vgamma9Vdelta2 T cell stimulation by a natural adenylated phosphoantigen. *J. Immunol.* **183**, 3848–3857 (2009).
- Scotet, E. *et al.* Tumor recognition following Vgamma9Vdelta2 T cell receptor interactions with a surface F1-ATPase-related structure and apolipoprotein A-I. *Immunity* **22**, 71–80 (2005).
- Mookerjee-Basu, J. *et al.* F1-adenosine triphosphatase displays properties characteristic of an antigen presentation molecule for Vgamma9Vdelta2 T cells. *J. Immunol.* **184**, 6920–6982 (2010).
- Champagne, E., Martinez, L. O., Vantourout, P., Collet, X. & Barbaras, R. Role of apolipoproteins in gammadelta and NKT cell-mediated innate immunity. *Immunol. Res.* **33**, 241–255 (2005).
- Hafiane, A. & Genest, J. HDL, atherosclerosis, and emerging therapies. *Cholesterol* **2013**, 891403 (2013).
- Shichiri, M. *et al.* ATP-binding cassette transporter A1 is involved in hepatic alpha-tocopherol secretion. *J. Nutr. Biochem.* **21**, 451–456 (2010).
- Berges, C. *et al.* A cell line model for the differentiation of human dendritic cells. *Biochem. Biophys. Res. Commun.* **333**, 896–907 (2005).
- Chan, W. K., Cheung, C. C., Law, H. K., Lau, Y. L. & Chan, G. C. Ganoderma lucidum polysaccharides can induce human monocytic leukemia cells into dendritic cells with immuno-stimulatory function. *J. Hematol. Oncol.* **1**, 9 (2008).
- dos Santos, G. G. *et al.* Progress on the development of human *in vitro* dendritic cell based assays for assessment of the sensitizing potential of a compound. *Toxicol. Appl. Pharmacol.* **236**, 372–382 (2009).
- Yamamoto, S. *et al.* Pharmacologic suppression of hepatic ATP-binding cassette transporter 1 activity in mice reduces high-density lipoprotein cholesterol levels but promotes reverse cholesterol transport. *Circulation* **124**, 1382–1390 (2011).
- Vedhachalam, C. *et al.* ABCA1-induced cell surface binding sites for apoA-I. *Arterioscler. Thromb. Vasc. Biol.* **27**, 1603–1609 (2007).
- Takahashi, K., Kimura, Y., Kioka, N., Matsuo, M. & Ueda, K. Purification and ATPase activity of human ABCA1. *J. Biol. Chem.* **281**, 10760–10768 (2006).
- Hozoji, M., Kimura, Y., Kioka, N. & Ueda, K. Formation of two intramolecular disulfide bonds is necessary for apoA-I-dependent cholesterol efflux mediated by ABCA1. *J. Biol. Chem.* **284**, 11293–11300 (2009).
- Costet, P., Luo, Y., Wang, N. & Tall, A. R. Sterol-dependent transactivation of the ABC1 promoter by the liver X receptor/retinoid X receptor. *J. Biol. Chem.* **275**, 28240–28245 (2000).
- Lee, J., Tauscher, A., Seo, D. W., Oram, J. F. & Kuver, R. Cultured gallbladder epithelial cells synthesize apolipoproteins A-I and E. *Am. J. Physiol. Gastrointest. Liver Physiol.* **285**, G630–G641 (2003).
- Gan, J. *et al.* Dual mechanisms of ABCA1 regulation by geranylgeranyl pyrophosphate. *J Biol Chem.* **276**, 48702–48708 (2001).
- Dong, F., Mo, Z., Eid, W., Courtney, K. C. & Zha, X. Akt inhibition promotes ABCA1-mediated cholesterol efflux to apoA-I through suppressing mTORC1. *PLoS One* **9**, e113789 (2014).
- Thurnher, M. & Gruenbacher, G. T lymphocyte regulation by mevalonate metabolism. *Sci. Signal.* **8**, re4 (2015).
- Okkenhaug, K. Signaling by the phosphoinositide 3-kinase family in immune cells. *Annu. Rev. Immunol.* **31**, 675–704 (2013).
- Riganti, C. *et al.* Zoledronic acid restores doxorubicin chemosensitivity and immunogenic cell death in multidrug-resistant human cancer cells. *PLoS ONE* **8**, e60975 (2013).
- Moriceau, G. *et al.* Zoledronic acid potentiates mTOR inhibition and abolishes the resistance of osteosarcoma cells to RAD001 (Everolimus): pivotal role of the prenylation process. *Cancer Res.* **70**, 10329–10334 (2010).
- Wang, J., Yang, X. & Zhang, J. Bridges between mitochondrial oxidative stress, ER stress and mTOR signaling in pancreatic  $\beta$  cells. *Cell Signal* **28**, 1099–1104 (2016).
- Lan, Y. C. *et al.* Zoledronic acid-induced cytotoxicity through endoplasmic reticulum stress triggered REDD1-mTOR pathway in breast cancer cells. *Anticancer Res.* **33**, 3807–3814 (2013).
- Ghavami, S. *et al.* Apoptosis, autophagy and ER stress in mevalonate cascade inhibition-induced cell death of human atrial fibroblasts. *Cell Death Dis.* **3**, e330 (2012).
- Tanaka, Y. *et al.* Natural and synthetic non-peptide antigens recognized by human gamma delta T cells. *Nature* **375**, 155–158 (1995).
- Gruenbacher, G. *et al.* Stress-related and homeostatic cytokines regulate  $V\gamma 9V\delta 2$  T cell surveillance of mevalonate metabolism. *Oncoimmunology* **3**, e953410 (2014).
- Rhodes, D. A. *et al.* Activation of human  $\gamma\delta$  T cells by cytosolic interactions of BTN3A1 with soluble phosphoantigens and the cytoskeletal adaptor periplakin. *J Immunol.* **194**, 2390–2398 (2015).
- Sandstrom, A. *et al.* The intracellular B30.2 domain of butyrophilin 3A1 binds phosphoantigens to mediate activation of human  $V\gamma 9V\delta 2$  T cells. *Immunity* **40**, 490–500 (2014).
- Riaño, F. *et al.*  $V\gamma 9V\delta 2$  TCR-activation by phosphorylated antigens requires butyrophilin 3 A1 (BTN3A1) and additional genes on human chromosome 6. *Eur. J. Immunol.* **44**, 2571–2576 (2014).
- Wang, H. & Morita, C. T. Sensor function for butyrophilin 3A1 in prenyl pyrophosphate stimulation of human  $V\gamma 2V\delta 2$  T Cells. *J. Immunol.* **195**, 4583–4594 (2015).
- De Libero, G., Lau, S. Y. & Mori, L. Phosphoantigen presentation to TCR  $\gamma\delta$  cells, a conundrum getting less gray zones. *Front. Immunol.* **5**, 679 (2015).
- Geyeregger, R. *et al.* Liver X receptors regulate dendritic cell phenotype and function through blocked induction of the actin-bundling protein fascin. *Blood* **109**, 4288–4295 (2007).
- Kilcollins, A. M., Li, J., Hsiao, C. H. & Wiemer, A. J. HMBPP analog prodrugs bypass energy-dependent uptake to promote efficient BTN3A1-mediated malignant cell lysis by Vgamma9Vdelta2 T lymphocyte effectors. *J. Immunol.* **197**, 419–428 (2016).
- Polakiewicz, R. D., Schieferl, S. M., Gingras, A. C., Sonenberg, N. & Comb, M. J. mu-Opioid receptor activates signaling pathways implicated in cell survival and translational control. *J. Biol. Chem.* **273**, 23534–23541 (1998).
- Li, S. & De Souza, P. Ras isoprenylation and pAkt inhibition by zoledronic acid and fluvastatin enhances paclitaxel activity in T24 bladder cancer cells. *Cancers (Basel)* **3**, 662–674 (2011).
- Hwahng, S. H., Ki, S. H., Bae, E. J., Kim, H. E. & Kim, S. G. Role of adenosine monophosphate-activated protein kinase-p70 ribosomal S6 kinase-1 pathway in repression of liver X receptor-alpha-dependent lipogenic gene induction and hepatic steatosis by a novel class of dithiolethiones. *Hepatology* **49**, 1913–1925 (2009).
- Mariani, S. *et al.* Effector gammadelta T cells and tumor cells as immune targets of zoledronic acid in multiple myeloma. *Leukemia* **19**, 664–670 (2005).
- Mandili, G. *et al.* Characterization of the protein ubiquitination response induced by Doxorubicin. *FEBS J.* **279**, 2182–2191 (2012).
- De Boo, S. *et al.* iNOS activity is necessary for the cytotoxic and immunogenic effects of doxorubicin in human colon cancer cells. *Mol. Cancer* **8**, 108 (2009).
- Campia, I. *et al.* Digoxin and ouabain induce the efflux of cholesterol via liver X receptor signalling and the synthesis of ATP in cardiomyocytes. *Biochem. J.* **447**, 301–311 (2012).
- Litman, T., Zeuthen, T., Skovsgaard, T. & Stein, W. D. Competitive, non-competitive and cooperative interactions between substrates of P-glycoprotein as measured by its ATPase activity. *Biochim. Biophys. Acta.* **1361**, 169–176 (1997).
- Kopecka, J. *et al.* Insights in the chemical components of liposomes responsible for P-glycoprotein inhibition. *Nanomedicine* **10**, 77–87 (2014).
- Beck, L. *et al.* The phosphate transporter PiT1 (Slc20a1) revealed as a new essential gene for mouse liver development. *PLoS ONE* **5**, e9148 (2010).
- Beltowski, J., Jamroz-Wisniewska, A., Nazar, J. & Wójcicka, G. Spectrophotometric assay of renal ouabain-resistant Na+ -ATPase and

- its regulation by leptin and dietary-induced obesity. *Acta Biochim. Pol.* **51**, 1003–1014 (2004).
54. Miraglia, E. *et al.* Na1/H1 exchanger activity is increased in doxorubicin-resistant human colon cancer cells and its modulation modifies the sensitivity of the cells to doxorubicin. *Int J Cancer.* **115**, 924–929 (2005).
55. Nagarajan, S. *et al.* Mechanical perturbations trigger endothelial nitric oxide synthase activity in human red blood cells. *Sci. Rep.* **6**, 26935 (2016).

### Acknowledgements

This study was supported by the Italian Association for Cancer Research (AIRC) (MFAG11475 and IG15232 to CR), (5 x mille n.12182 and IG 15257 to FN), (IG 13119 and IG 16985 to MM); PRIN 2010NECHBX\_002 to MM; Compagnia San Paolo-University of Turin to FN; Progetti Ateneo (2014-PC\_METHAIMMUNOTHER and 2011-RETTE to FN); Fondazione Ricerca Molinette to F.N. B.C., M.F. and J.K. are post-doc research fellows supported by PRIN (BC), AIRC (MF), and Fondazione Umberto Veronesi (JK). We are grateful to Prof. Amalia Bosia and Prof. Dario Ghigo (Dipartimento di Oncologia, Università di Torino) for their fruitful discussions and to Mr. Costanzo Costamagna (Dipartimento di Oncologia, Università di Torino) for his technical assistance. We are also grateful to Mr. Andrew Martin Garvey, BAHons LTCL(TESOL) PGDip MA for his editorial assistance.

### Author contributions

B.C., C.R. and M.M. designed the study, analysed the data and drafted the manuscript. B.C. and J.K. performed the experiments and analysed the data. P.S., G.M. and M.F. assisted with the experiments and analysed the data. N.M. and D.C. conceived the working hypothesis, contributed to the data analysis and revised the manuscript. B.C., F.N., C.R. and M.M. interpreted the data, revised the manuscript and obtained funding. B.C., C.R. and M.M. supervised the study and finalized the submission.

### Additional information

**Supplementary Information** accompanies this paper at <http://www.nature.com/naturecommunications>

**Competing interests:** The authors declare no competing financial interests.

**Reprints and permission** information is available online at <http://npg.nature.com/reprintsandpermissions/>

**How to cite this article:** Castella, B. *et al.* The ATP-binding cassette transporter A1 regulates phosphoantigen release and V $\gamma$ 9V $\delta$ 2 T cell activation by dendritic cells. *Nat. Commun.* **8**, 15663 doi: 10.1038/ncomms15663 (2017).

**Publisher's note:** Springer Nature remains neutral with regard to jurisdictional claims in published maps and institutional affiliations.



**Open Access** This article is licensed under a Creative Commons Attribution 4.0 International License, which permits use, sharing, adaptation, distribution and reproduction in any medium or format, as long as you give appropriate credit to the original author(s) and the source, provide a link to the Creative Commons license, and indicate if changes were made. The images or other third party material in this article are included in the article's Creative Commons license, unless indicated otherwise in a credit line to the material. If material is not included in the article's Creative Commons license and your intended use is not permitted by statutory regulation or exceeds the permitted use, you will need to obtain permission directly from the copyright holder. To view a copy of this license, visit <http://creativecommons.org/licenses/by/4.0/>

© The Author(s) 2017